1,3-Dipolar Cycloaddition to the Fe–N=C Fragment. 11.[1] Isocyanide-Controlled Change between a Reversible Molecular Self-Assembly of Three Components, Including a Unique Isocyanide Deinsertion, and Dimethyl Maleate Coupling Reactions

Paul P. M. de Lange, René P. de Boer, Maarten van Wijnkoop, Jan M. Ernsting, Hans-Werner Frühauf,* and Kees Vrieze

Laboratorium voor Anorganische Chemie, J. H. van 't Hoff Instituut, Universiteit van Amsterdam, Nieuwe Achtergracht 166, 1018 WV Amsterdam, The Netherlands

Wilberth J. J. Smeets and Anthony L. Spek

Bijvoet Center for Biomolecular Research, Vakgroep Kristal-en Structuurchemie, Rijksuniversiteit Utrecht, Padualaan 8, 3584 CH Utrecht, The Netherlands

Kees Goubitz

Laboratorium voor Kristallografie, J. H. van 't Hoff Instituut, Universiteit van Amsterdam, Nieuwe Achtergracht 166, 1018 WV Amsterdam, The Netherlands

Received August 10, 1992

In the reaction of $Fe(CNR)_3$(*i*-Pr-α-diimine) (**6**; R = 2,6-xylyl (**a**), *t*-Bu (**b**), c-Hex (**c**)) with dimethyl maleate, two totally different pathways are followed, depending on the type of isocyanide used. With the aromatic isocyanide, a 1,3-dipolar cycloaddition of the alkene to the Fe—N=C unit occurs followed by an isocyanide insertion, forming a ferra [2.2.2] bicyclic compound (**7a**). When this mixture is warmed above room temperature, the reaction is reversed, disassembling **7a** into its starting components. During this facile retro-cycloaddition, C—C, C—N, and Fe—C bonds are broken. Also, the first unambiguous example of an isocyanide deinsertion is encountered. The starting complexes **6b,c**, with aliphatic isocyanides, react with dimethyl maleate to give two products. The first, a purely organic product (**8**), is a dimer of two coupled alkenes. The second product is the organometallic tricyclic complex $Fe(CNR)_3$(tric) (**9b,c**), in which two alkenes are coupled and bonded to the metal and the α-diimine ligand. In the cyclization reaction, a γ-lactam ring is formed and a methoxy group of one of the four ester groups is removed, with formation of methanol. The molecular structure of the [2.2.2] bicyclic complex **7a** ($FeC_{50}H_{60}N_6O_4$, triclinic, space group $P\bar{1}$, a = 10.367 (1) Å, b = 14.615 (3) Å, c = 15.787 (2) Å, α = 95.78 (2)°, β = 96.62 (1)°, γ = 92.21 (1)°, Z = 2, R = 0.053, R_w = 0.055) consists of three six-membered rings with the metal in a bridgehead position. The single-crystal X-ray structure of the organic dimer **8** ($C_{12}H_{16}O_8$, monoclinic, space group $A2/a$, a = 8.291 (2) Å, b = 8.291 (2) Å, c = 20.551 (2) Å, β = 96.09 (1)°, Z = 4, R = 0.068, R_w = 0.089) reveals a symmetric alkene. The molecular structure of the Fe(*t*-BuNC)$_3$(tric) species **9b** ($FeC_{34}H_{55}N_5O_7 \cdot 0.5CH_2Cl_2 \cdot 0.5C_4H_{10}O$, monoclinic, space group Pc, a = 11.201 (1) Å, b = 12.251 (2) Å, c = 32.019 (3) Å, β = 96.43 (1)°, Z = 4, R = 0.0581, R_w = 0.0629) consists of a four-, a five-, and a six-membered ring. The metal is incorporated in the six- and the four-membered rings.

Introduction

Organometallic reactions involving C–C coupling and fission, such as dimerization, poly- and oligomerization, and metathesis, are of particular interest. This interest originates from both fundamental and theoretical points of view and from the relation to industrial processes such as Ziegler–Natta and Fischer–Tropsch.[2]

With complexes containing DAB[3a] ligands, C–C bond formation reactions have been described with unsaturated substrates such as diimides,[4] sulfines,[4] α-diimines,[5] and alkynes.[6] In all of these reactions coupling to the DAB imine carbon atom occurred. Besides stoichiometric reactions, catalysis was also observed in the cyclotrimerization of electron-deficient alkynes by a palladacyclopentadiene (DAB) complex.[7]

* To whom correspondence should be addressed.

(1) (a) Part of this work has been published in preliminary form: de Boer, R. P.; de Lange, P. P. M.; Frühauf, H.-W.; Vrieze, K. *J. Chem. Soc., Chem. Commun.* **1992**, 580. (b) Part 10: de Lange, P. P. M.; van Wijnkoop, M.; Frühauf, H.-W.; Vrieze, K. *Organometallics*, preceding paper in this issue.

(2) (a) Muetterties, E. L.; Stein, J. J. *Chem. Rev.* **1979**, *79*, 479. (b) Brady, R. C.; Pettit, R. *J. Am. Chem. Soc.* **1981**, *103*, 1287. (c) Leconte, M.; Basset, J. M.; Quingard, F.; Laroche, C. In *Reactions of Coordinated Ligands*; Braterman, P. S., Ed.; Plenum Press: New York, London, 1986; Vol. 1, p 371. (d) Pines, H. In *The Chemistry of Catalytic Hydrocarbon Conversions*; Academic Press: New York, 1981. (e) Masters, C. In *Homogeneous Transition-Metal Catalysis*; Chapman and Hall: New York, 1981.

(3) (a) The 1,4-diaza 1,3-dienes of formula R'N=CHCH=NR' are abbreviated as R'-DAB. (b) The [2.2.2] bicyclic structure is abbreviated as bic. (c) The tricyclic structures are abbreviated as tric.

0276-7333/93/2312-0440$04.00/0

Scheme I. Cycloaddition of $Fe(CO)_{3-n}(CNR)_n(DAB)$ (n = 0, 1, 3) to DMAD

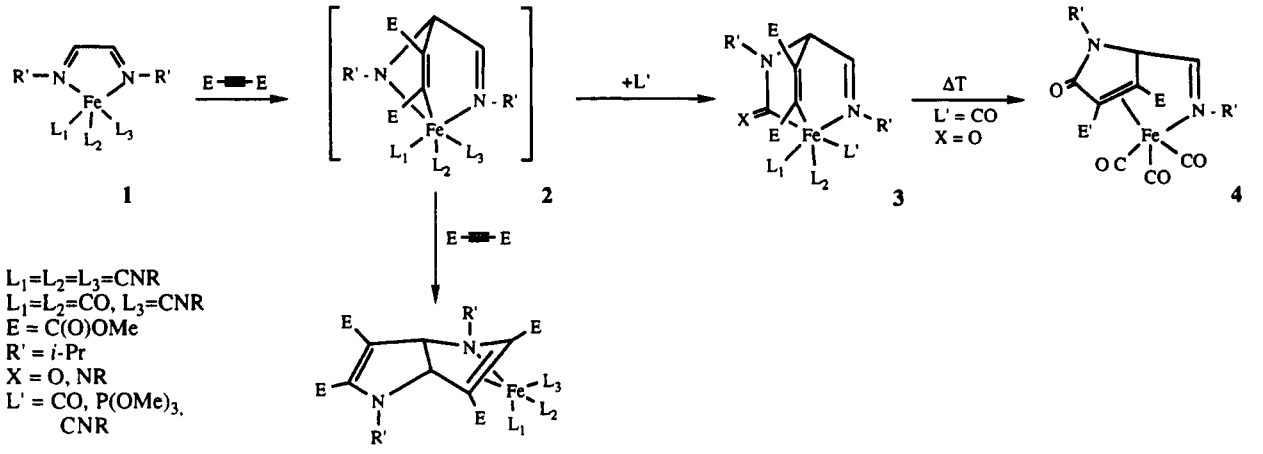

One of the reactions which has drawn our special attention is the reaction of $M(CO)_{3-n}(CNR)_n(DAB)$ complexes (M = Fe, Ru; n = 0, 1, and 3) with activated alkynes. In this reaction, described as an oxidative 1,3-dipolar [3 + 2] cycloaddition, the alkyne adds across the Fe—N=C unit of complex **1** to give an intermediate [2.2.1] bicyclic structure (**2**; see Scheme I). The intermediate **2** undergoes an insertion reaction leading to a stable [2.2.2] bicyclic complex (**3**). For n = 0, isomerization via a reductive elimination followed by recoordination of the π bond leads to the formation of a 1,5-dihydropyrrol-2-one complex (**4**).[8,9] When one of the three CO ligands of the starting complex **1** was substituted for a better σ-donating/worse π-accepting[10,11] isocyanide ligand, the Fe^{II}—N=C unit in the [2.2.1] intermediate **2** was sufficiently activated to again undergo a 1,3-dipolar cycloaddition, finally leading to the formation of a tetrahydropyrrolopyrrole complex (**5**).[9] In a previous paper[1b] we described the synthesis of highly activated $Fe(CNR)_3(DAB)$ complexes (**6**). These complexes proved to show a reactivity toward alkynes analogous to that for the $Fe(CO)_{3-n}(CRN)_n(DAB)$ (n = 0, 1) complexes.

In this article we discuss the fascinating reactivity of $Fe(CNR)_3(DAB)$ toward dimethyl maleate (DMM).

Experimental Section

Materials and Apparatus. The ^1H and ^{13}C NMR spectra were recorded on Bruker AC 100 and AMX 300 spectrometers. IR spectra were obtained on a Perkin-Elmer 283 spectrophotometer. All experiments were performed under a nitrogen atmosphere, using standard Schlenk techniques. The solvents were dried and distilled under nitrogen before use. Column chromatography was carried out using silanized silica gel 60 (Merck, 70–230 mesh), activated before use as the stationary phase.[12] Elemental analyses were carried out by Dornis und Kolbe, Mikroanalytisches Laboratorium, Mülheim a. d. Ruhr, Germany. 2,6-Xylyl (**a**), *tert*-butyl (**b**), and cyclohexyl (**c**) isocyanides (Fluka) and dimethyl maleate (Janssen) were obtained commerically and used without purification. $Fe(CNR)_3$-(*i*-Pr-DAB) (**6**) was prepared according to known procedures.[1b,13]

Formation of Fe(2,6-xylylNC)$_3$([2.2.2]bic)[3b] (7a). A solution of $Fe(2,6\text{-xylylNC})_3$(*i*-Pr-DAB) (**6a**; 710 mg, 1.20 mmol) and 1 equiv of 2,6-xylyl isocyanide (**a**; 160 mg, 1.20 mmol) in 30 mL of pentane was prepared in situ. To this solution was added at room temperature, over a period of 1 h, a solution of DMM (170 mg, 1.20 mmol) in 5 mL of Et_2O and 10 mL of pentane, and the mixture was then stirred for 2 h. The resulting yellow precipitate was washed three times with 15 mL of pentane and dried in vacuo. The yield of $Fe(2,6\text{-xylylNC})_3$([2.2.2]bic) (**7a**) is 95%. The product could be further purified by means of crystallization, at room temperature, from a concentrated Et_2O/CH_2Cl_2 (3/5) solution by slow diffusion of hexane.

Formation of Tetramethyl 2-Butene-1,2,3,4-tetracarboxylate (TMBC) (8) and Fe(CNR)$_3$(tric)[3c] (9b,c). To an in situ prepared solution of $Fe(CNR)_3$(*i*-Pr-DAB) (**6b,c**; 1.0 mmol) in 20 mL of pentane was added a solution of DMM (290 mg, 2.0 mmol) in 5 mL of Et_2O and 10 mL of pentane at 273 or 243 K over a period of 1 h, and this mixture was subsequently stirred for an additional 2 h. The yellow precipitate was washed three times with 15 mL of pentane, dried in vacuo, dissolved in Et_2O/CH_2Cl_2 (5/1), and separated by column chromatography. The column was prepared with pentane. Elution with Et_2O afforded a yellow band, containing the organic TMBC (**8**). Further elution with Et_2O/CH_2Cl_2 (5/1) yielded a second yellow band, which after evaporation of the solvent gave $Fe(CNR)_3$(tric) (**9b,c**) as a yellow powder. The product ratios of TMBC (**8**)/$Fe(CNR)_3$(tric) (**9b,c**) were 20/80 at 243 K and 60/40 at 273 K. The total yield of TMBC and $Fe(CNR)_3$(tric) (**9b,c**) was 50%. Crystals of both TMBC (**8**) and $Fe(CNR)_3$(tric) (**9b,c**) were grown from a concentrated Et_2O/CH_2Cl_2 (5/1) solution at −30 °C.

(4) Keijsper, J.; Polm, L. H.; van Koten, G.; Vrieze, K.; Stam, C. H.; Schagen, J. D. *Inorg. Chim. Acta* **1985**, *103*, 137.
(5) (a) Staal, L. H.; Polm, L. H.; Balk, R. W.; van Koten, G.; Vrieze, K.; Brouwers, A. M. F. *Inorg. Chem.* **1980**, *19*, 3343. (b) Keijsper, J.; Polm, L. H.; van Koten, G.; Vrieze, K.; Abbel, G.; Stam, C. H. *Inorg. Chem.* **1984**, *23*, 2142.
(6) (a) Staal, L. H.; van Koten, G.; Vrieze, K.; van Santen, B.; Stam, C. H. *Inorg. Chem.* **1981**, *20*, 3598. (b) Muller, F.; Dijkhuis, D. I. P.; van Koten, G.; Vrieze, K.; Heijdenrijk, D.; Rotteveel, M. A.; Stam, C. H.; Zoutberg, M. C. *Organometallics* **1989**, *8*, 992.
(7) tom Dieck, H.; Munz, C.; Müller, C. *J. Organomet. Chem.* **1990**, *384*, 243.
(8) (a) Frühauf, H.-W.; Seils, F.; Goddard, R. J.; Romão, M. J. *Angew. Chem.* **1983**, *95*, 1014. (b) Frühauf, H.-W.; Seils, F.; Romão, M. J.; Goddard, R. J. *Organometallics* **1985**, *4*, 948. (c) Frühauf, H.-W.; Seils, F. *J. Organomet. Chem.* **1986**, *302*, 59. (d) Frühauf, H.-W.; Seils, F. *J. Organomet. Chem.* **1987**, *323*, 67. (e) Frühauf, H.-W.; Seils, F.; Stam, C. H. *Organometallics* **1989**, *8*, 2338. (f) van Wijnkoop, M.; de Lange, P. P. M.; Frühauf, H.-W.; Vrieze, K.; Wang, Y.; Goubitz, K.; Stam, C. H. *Organometallics* **1992**, *11*, 3607.
(9) (a) de Lange, P. P. M.; Frühauf, H.-W.; van Wijnkoop, M.; Vrieze, K.; Wang, Y.; Heijdenrijk, D.; Stam, C. H. *Organometallics* **1990**, *9*, 1691. (b) de Lange, P. P. M.; Frühauf, H.-W.; Kraakman, M. J. A.; van Wijnkoop, M.; Kranenburg, M.; Groot, A. H. J. P.; Vrieze, K.; Fraanje, J.; Wang, Y.; Numan, M. *Organometallics*, first of the three successive papers in this issue.
(10) (a) Yamamoto, Y. *Coord. Chem. Rev.* **1980**, *32*, 193. (b) Bonati, F.; Minghetti, G. *Inorg. Chim. Acta* **1974**, *9*, 95. (c) Carmona, E.; Galindo, E.; Matin, J. M. *Polyhedron* **1988**, *7*, 1831. (d) Bassett, J. N.; Green, M.; Howard, J. A. K.; Stone, F. G. A. *J. Chem. Soc., Dalton Trans.* **1979**, 1003.
(11) (a) Yamamoto, Y.; Yamazaki, H. *Coord. Chem. Rev.* **1972**, *8*, 225. (b) Treichel, P. M. *Adv. Organomet. Chem.* **1973**, *11*, 21. (c) Singleton, E.; Oosthuizen, H. E. *Adv. Organomet. Chem.* **1983**, *22*, 209.
(12) The use of normal, not silanized, silica gel leads to nearly complete decomposition of the products.
(13) tom Dieck, H.; Diercks, R.; Stamp, L.; Bruder, H.; Schuld, T. *Chem. Ber.* **1987**, *120*, 1943.

Table I. Crystal Data and Details of the Structure Determination of Fe(2,6-xylylNC)$_3$([2.2.2]bic) (7a), TMBC (8), and Fe(*t*-BuNC)$_3$(tric) (9b)

	7a	8	9b
		Crystal Data	
formula	$FeC_{50}H_{60}N_6O_4$	$C_{12}H_{16}O_8$	$FeC_{34}H_{55}N_5O_7 \cdot 0.5CH_2Cl_2 \cdot 0.5C_4H_{10}O$
mol wt	864.9	288.3	781.22
cryst syst	triclinic	monoclinic	monoclinic
space group	$P\bar{1}$	$A2/a$	Pc
a, b, c (Å)	10.367 (1), 14.615 (3), 15.787 (2)	8.291 (2), 8.662 (5), 20.551 (2)	11.201 (1), 12.251 (2), 32.019 (3)
α, β, γ (deg)	95.78 (2), 96.62 (1), 92.21 (1)	90, 96.09 (1), 90	90, 96.43 (1), 90
V (Å^3)	2360.9 (9)	1467.5 (4)	4366.1 (9)
Z	2	4	4
D_{calc} (g cm^{-3})	1.22	1.3	1.188
$F(000)$	920	608	1.672
μ (cm^{-1})	29.3 (Cu Kα)	9.2 (Cu Kα)	4.7 (Mo Kα)
cryst size (mm)	0.20 × 0.60 × 0.80	0.40 × 0.45 × 0.55	0.20 × 0.30 × 0.38
		Data Collection	
temp (K)	295	295	295
$\theta_{min}, \theta_{max}$ (deg)	2.8, 65	4.5, 75	0.64, 25.4
radiation	Cu Kα (1.5418 Å)	Cu Kα (1.5418 Å)	Mo Kα (0.710 73 Å)
scan type	θ–2θ	θ–2θ	ω–2θ
$\Delta\omega$ (deg)	1.2 + 0.15 tan θ	1.2 + 0.15 tan θ	0.73 + 0.35 tan θ
ref rflns	–1,2,–2; –1,0,0	–1,2,2; –1,0,0	230; 1,2,–7; 402
total no. of data	8190	3222	12 653
total no. of unique data	8005	1505	10 103
no. of obs data	5743 ($I > 2.5\sigma(I)$)	1364 ($I > 2.5\sigma(I)$)	3709 ($I > 2.5\sigma(I)$)
		Refinement	
DIFABS cor range	0.67, 1.82	0.70, 1.48	
no. of refined params	792	247	875
final R, R_w, S	0.053, 0.055, 1.38	0.068, 0.089, 0.27	0.058, 0.063, 2.03
$(\Delta/\sigma)_{max}$ in final cycle	0.88	0.62	0.005
min and max resd dens, (e Å^{-3})	–0.4, +0.4	–0.2, +0.2	–0.33, +0.52

^{1}H NMR Experiment. Fe(2,6-xylylNC)$_3$([2.2.2]bic) (**7a**; 5 mg, 5.8 × 10^{-3} mmol) was dissolved in C_6D_6 (0.5 mL) in a standard 5-mm NMR tube. The temperature was raised to 333 K, and the reaction was monitored periodically. After the complete disappearance of **7a** (ca. 1.5 h) the temperature was reduced to room temperature and the reaction was followed again.

Crystal Structure Determination of Fe(2,6-xylylNC)$_3$([2.2.2]bic) (7a). A crystal with the approximate dimensions 0.20 × 0.60 × 0.80 mm^3 was used for data collection on an Enraf-Nonius CAD-4 diffractometer with graphite-monochromated Cu Kα radiation and θ–2θ scan. A total of 8005 unique reflections was measured within the range $-12 \le h \le 0$, $-17 \le k \le 17$, $-18 \le l \le 18$. Of these, 5743 were above the significance level of $2.5\sigma(I)$. The maximum value of $(\sin\theta/\lambda)$ was 0.59 Å^{-1}. Unit-cell parameters were refined by a least-squares fitting procedure using 23 reflections with $80 < 2\theta < 84°$. Corrections for Lorentz and polarization effects were applied. About half of the structure was found by direct methods. After isotropic refinement the remainder of the non-hydrogen atoms was found in a ΔF synthesis. The hydrogen atom positions were calculated. Block-diagonal least-squares refinement on F, anisotropic for the non-hydrogen atoms and isotropic for the hydrogen atoms, with restraint on the latter in such a way that the distance to their carrier remained constant at approximately 1.09 Å, converged to $R = 0.053$, $R_w = 0.055$, and $(\Delta/\sigma)_{max} = 0.88$. The weighting scheme $w = (7.6 + F_o + 0.008F_o^2)^{-1}$ was used. Am empirical absorption correction (DIFABS[14]) was applied, with correction coefficients in the range of 0.67–1.82. The secondary isotropic extinction coefficient was refined to $g = 4.3 \times 10^2$.[15,16] A final difference Fourier map revealed a residual electron density between –0.4 and +0.4 e Å^{-3}. Scattering factors were taken from Cromer and Mann.[17] The anomalous scattering of Fe was taken into account. All calculations were performed with XTAL[18] unless stated otherwise. Crystal data and numerical details of the structure determination are given in Table I. Final atomic coordinates and equivalent isotropic thermal parameters of the non-hydrogen atoms are listed in Table II.

Crystal Structure Determination of TMBC (8). A crystal with the approximate dimensions 0.40 × 0.45 × 0.55 mm^3 was used for data collection on an Enraf-Nonius CAD-4 diffractometer with graphite-monochromated Cu Kα radiation and θ–2θ scan. A total of 1505 unique reflections was measured within the range $-0 \le h \le 10$, $0 \le k \le 10$, $-25 \le l \le 25$. Of these, 1364 were above the significance level of $2.5\sigma(I)$. The maximum value of $(\sin\theta)/\lambda$ was 0.63 Å^{-1}. Unit-cell parameters were refined by a least-squares fitting procedure using 23 reflections with $80 < 2\theta < 90°$. Corrections for Lorentz and polarization effects were applied. The structure was solved by direct methods using the program Simpel.[19] The hydrogen atom positions were calculated. Block-diagonal least-squares refinement on F, anisotropic for the non-hydrogen atoms and isotropic for the hydrogen atoms, converged to $R = 0.068$, $R_w = 0.089$, and $(\Delta/\sigma)_{max} = 0.62$. The weighting scheme $w = (4.1 + F_o + 0.003F_o^2)^{-1}$ was used. An empirical absorption correction (DIFABS[14]) was applied, with correction coefficients in the range 0.70–1.48. A final difference Fourier map revealed a residual electron density between –0.2 and +0.2 e Å^{-3}. The isotropic secondary extinction coefficient was refined to $g = [2.6\ (9)] \times 10^2$.[15,16] Scattering factors were taken from Cromer and Mann.[17] All calculations were performed with XTAL,[18] unless stated otherwise. Crystal data and numerical details of the structure determination are listed in Table I. Final atomic coordinates and equivalent isotropic thermal parameters of the non-hydrogen atoms are given in Table III.

Crystal Structure Determination of Fe(*t*-BuNC)$_3$(tric) (9b). A red-brown block-shaped crystal was mounted on top of a glass fiber and transferred to an Enraf-Nonius CAD4T

(14) Walker, N.; Stuart, D. *Acta Crystallogr.* **1983**, *A39*, 158.
(15) Zachariasen, W. H. *Acta Crystallogr.* **1967**, *A23*, 558.
(16) Larson, A. C. The inclusion of secondary extinction in least-squares refinement crystal structures. In *Crystallographic Computing*; Ahmed, F. R., Hall, S. R., Huber, C. P. Eds.; Munksgaard: Copenhagen, Denmark, 1969; p 291.
(17) (a) Cromer, D. T.; Mann, J. B. *Acta Crystallogr.* **1968**, *A24*, 321. (b) Cromer, D. T.; Mann, J. B. In *International Tables for X-ray Crystallography*; Kynoch Press: Birmingham, England, 1974; Vol. IV, p 55.
(18) *XTAL2.6 User's Manual*; Hall, S. R., Stewart, J. M., Eds.; Universities of Western Australia and Maryland.
(19) Schenk, H.; Hall, S. R. SIMPEL. In *XTAL3.0 User's Manual*; Hall, S. R., Stewart, J. M., Eds.; Universities of Western Australia and Maryland.

Table II. Fractional Coordinates of the Non-Hydrogen Atoms and Equivalent Isotropic Thermal Parameters for Fe(2,6-xylylNC)$_3$([2.2.2]bic) (7a) (Esd's in Parentheses)

atom	x	y	z	U_{eq} (Å^2)[a]
Fe	0.22796 (6)	0.72010 (4)	0.29477 (4)	0.0290 (3)
C1	0.1760 (4)	0.8504 (3)	0.2911 (2)	0.036 (2)
C2	0.2604 (4)	0.8730 (3)	0.4423 (3)	0.045 (2)
C3	0.1569 (4)	0.8065 (3)	0.4687 (3)	0.043 (2)
C4	0.1316 (4)	0.7159 (3)	0.4086 (2)	0.034 (2)
C5	0.3829 (4)	0.8285 (3)	0.4337 (3)	0.043 (2)
C6	0.2454 (5)	1.0107 (3)	0.3585 (3)	0.059 (3)
C7	0.3930 (6)	1.0278 (4)	0.3720 (4)	0.091 (4)
C8	0.1782 (8)	1.0741 (4)	0.4205 (4)	0.107 (5)
C9	0.5170 (4)	0.7199 (3)	0.3657 (3)	0.049 (3)
C10	0.6069 (5)	0.7849 (4)	0.3286 (4)	0.089 (4)
C11	0.5790 (5)	0.6913 (4)	0.4504 (4)	0.080 (4)
C12	0.1878 (5)	0.7935 (3)	0.5617 (3)	0.058 (3)
C13	0.1112 (8)	0.7255 (4)	0.6783 (3)	0.107 (5)
C14	0.1774 (4)	0.6360 (3)	0.4478 (2)	0.038 (2)
C15	0.1445 (5)	0.4742 (3)	0.4530 (3)	0.062 (3)
C16	0.0709 (4)	0.6873 (2)	0.2354 (2)	0.033 (2)
C17	0.2678 (3)	0.5965 (3)	0.2865 (2)	0.033 (2)
C18	0.3017 (4)	0.7374 (3)	0.1977 (2)	0.036 (2)
C31	0.0485 (4)	0.9521 (3)	0.2014 (3)	0.040 (2)
C32	−0.0690 (4)	0.9706 (3)	0.2346 (3)	0.055 (3)
C33	−0.1452 (5)	1.0389 (3)	0.2021 (4)	0.070 (3)
C34	−0.1089 (5)	1.0871 (3)	0.1374 (4)	0.071 (4)
C35	0.0063 (5)	1.0686 (3)	0.1047 (3)	0.059 (3)
C36	0.0852 (4)	1.0019 (3)	0.1361 (3)	0.046 (2)
C37	−0.1135 (6)	0.9153 (4)	0.3033 (4)	0.087 (4)
C38	0.2107 (5)	0.9818 (4)	0.0992 (3)	0.067 (3)
C41	−0.1588 (4)	0.6417 (3)	0.1606 (3)	0.043 (2)
C42	−0.2330 (4)	0.5783 (3)	0.1972 (3)	0.055 (3)
C43	−0.3576 (5)	0.5528 (4)	0.1557 (4)	0.077 (4)
C44	−0.4014 (5)	0.5896 (4)	0.0824 (4)	0.085 (4)
C45	−0.3275 (6)	0.6528 (4)	0.0477 (4)	0.079 (4)
C46	−0.2027 (5)	0.6817 (3)	0.0875 (3)	0.056 (3)
C47	−0.1828 (5)	0.5392 (4)	0.2785 (4)	0.076 (4)
C48	−0.1225 (6)	0.7547 (4)	0.0538 (3)	0.081 (4)
C51	0.2986 (4)	0.4228 (3)	0.2625 (3)	0.038 (2)
C52	0.4025 (4)	0.3859 (3)	0.3081 (3)	0.051 (3)
C53	0.4093 (6)	0.2902 (4)	0.2994 (3)	0.073 (4)
C54	0.3158 (7)	0.2367 (3)	0.2465 (4)	0.089 (4)
C55	0.2147 (6)	0.2747 (3)	0.2016 (4)	0.078 (4)
C56	0.2042 (5)	0.3698 (3)	0.2080 (3)	0.053 (3)
C57	0.5017 (5)	0.4470 (4)	0.3667 (4)	0.078 (4)
C58	0.0941 (6)	0.4115 (4)	0.1583 (4)	0.084 (4)
C61	0.3643 (4)	0.7529 (3)	0.0478 (3)	0.050 (3)
C62	0.4507 (5)	0.8200 (4)	0.0269 (3)	0.066 (3)
C63	0.4641 (6)	0.8217 (4)	−0.0605 (4)	0.088 (5)
C64	0.2955 (7)	0.7598 (5)	−0.1201 (4)	0.100 (5)
C65	0.3134 (6)	0.6926 (5)	−0.0982 (4)	0.087 (4)
C66	0.2949 (5)	0.6876 (4)	−0.0131 (3)	0.062 (3)
C67	0.5295 (6)	0.8844 (4)	0.0940 (4)	0.087 (4)
C68	0.2091 (5)	0.6129 (4)	0.0131 (4)	0.078 (4)
N1	0.2096 (3)	0.9120 (2)	0.3638 (2)	0.043 (2)
N2	0.3880 (3)	0.7620 (2)	0.3734 (2)	0.038 (2)
N3	0.1164 (3)	0.8745 (2)	0.2202 (2)	0.040 (2)
N4	−0.0327 (3)	0.6659 (2)	0.2010 (2)	0.041 (2)
N5	0.2885 (3)	0.5182 (2)	0.2825 (2)	0.039 (2)
N6	0.3444 (3)	0.7499 (2)	0.1338 (2)	0.048 (2)
O1	0.2841 (4)	0.8242 (3)	0.6087 (2)	0.086 (3)
O2	0.0891 (4)	0.7466 (2)	0.5895 (2)	0.068 (2)
O3	0.2737 (3)	0.6326 (2)	0.4992 (2)	0.052 (2)
O4	0.1014 (3)	0.5578 (2)	0.4191 (2)	0.047 (2)

[a] $U_{eq} = {}^1/_3\sum_i\sum_j U_{ij}a_i^*a_j^*\mathbf{a}_i\mathbf{a}_j$.

diffractometer (rotating anode, 50 kV, 200 mA, graphite-monochromated Mo Kα radiation) for data collection. Unit cell parameters were determined from a least-squares treatment of the SET4 setting angles of 25 reflections with $11.2 < \theta < 13.7°$. The unit cell parameters were checked for the presence of higher lattice symmetry.[20] The crystals reflected poorly; reflection profiles were rather broad. A total of 12 653 intensity data was collected in the range $-13 \le h \le +13$, $0 \le k \le 14$, $-38 \le l \le +38$. Data were corrected for Lp and for a linear decay (50%) of the intensity control reflections during 39 h of X-ray exposure time but not for the absorption. The structure was solved with standard Patterson methods (SHELXS86[21]) and a series of subsequent difference Fourier analyses. Refinement on F was carried out by full-matrix least-squares techniques. H atoms were introduced on calculated positions (C–H = 0.98 Å) and included in the refinement riding on their carrier atoms. All non-H atoms were refined with anisotropic thermal parameters; H atoms were refined with common isotropic thermal parameters (U = 0.042 (11), 0.060 (16), and 0.139 (8) Å^2 for –CH, –CH$_2$, and –CH$_3$ groups, respectively). A Et$_2$O solvate molecule could not be located from difference Fourier maps unambiguously and was taken into account in the structure factor and refinement calculations by direct Fourier transformation of the electron density in the cavity, by following the BYPASS procedure.[22] Weights were introduced in the final refinement cycles; convergence was reached at R = 0.0581 and R_w = 0.0629 ($w = 1/[\sigma^2(F) + 0.00117F^2]$). The absolute structure was checked by refinement with opposite f'' anomalous scattering factors, resulting in R = 0.0605 and R_w = 0.0651. Crystal data and numerical details of the structure determination are given in Table I. Final atomic coordinates and equivalent isotropic thermal parameters are listed in Table IV. Neutral atom scattering factors were taken from Cromer and Mann[17a] and corrected for anomalous dispersion.[23] All calculations were performed with SHELX76[24] and PLATON[25] (geometrical calculations and illustrations) on either a MicroVAX-II cluster or a DEC-5000 workstation.

Table III. Fractional Coordinates of the Non-Hydrogen Atoms and Equivalent Isotropic Thermal Parameters for TMBC (8) (Esd's in Parentheses)

atom	x	y	z	U_{eq} (Å^2)[a]
C1	0.2501 (2)	0.5611 (2)	0.4708 (1)	0.045 (1)
C2	0.1498 (3)	0.7103 (3)	0.4388 (1)	0.051 (1)
C3	0.2233 (4)	0.9573 (4)	0.4051 (2)	0.084 (2)
C4	0.1438 (3)	0.4196 (3)	0.4336 (1)	0.050 (1)
C5	0.1987 (3)	0.4149 (3)	0.3661 (1)	0.053 (1)
C6	0.2234 (7)	0.2586 (6)	0.2742 (2)	0.116 (3)
O1	0.0104 (2)	0.7362 (2)	0.4203 (1)	0.071 (1)
O2	0.2710 (2)	0.8081 (2)	0.4328 (1)	0.060 (1)
O3	0.2647 (3)	0.5197 (3)	0.3414 (1)	0.079 (1)
O4	0.1657 (3)	0.2789 (2)	−0.33808 (9)	0.068 (1)

[a] $U_{eq} = {}^1/_3\sum_i\sum_j U_{ij}a_i^*a_j^*\mathbf{a}_i\mathbf{a}_j$.

Results

The ligands and complexes employed are shown in Scheme II. The three different isocyanides are differentiated by letters (2,6-xylyl (**a**), *t*-Bu (**b**), and c-Hex (**c**)); the type of complex is identified by boldface arabic numbers. In the reaction of Fe(CNR)$_3$(*i*-Pr-DAB) (**6**) with the electron-deficient alkene dimethyl maleate three different products were formed. The product distribution is governed by the type of isocyanide used. With the aromatic 2,6-xylyl isocyanide complex **6a** a [3 + 2] cycloaddition reaction, leading to the [2.2.2] bicyclic complex **7a**, occurs. When slightly warmed in solution, this [2.2.2] bicyclic compound undergoes consecutive deinsertion and cycloreversion reactions, yielding the starting compounds.

In the case of the aliphatic *tert*-butyl and cyclohexyl isocyanides **6b,c** two products were formed, the organo-

(20) Spek, A. L. *J. Appl. Crystallogr.* **1988**, *21*, 578.

(21) Sheldrick, G. M. SHELXS86: Program for Crystal Structure Determination; University of Göttingen: Göttingen, Federal Republic of Germany, 1986.

(22) van der Sluis, P.; Spek, A. L. *Acta Crystallogr.* **1990**, *A46*, 194.

(23) Cromer, D. T.; Liberman, D. *J. Chem. Phys.* **1970**, *53*, 1891.

(24) Sheldrick, G. M. SHELX76: Crystal Structure Analysis Package; University of Cambridge, Cambridge, England, 1976.

(25) Spek, A. L. *Acta Crystallogr.* **1990**, *A46*, C34.

Table IV. Fractional Coordinates of the Non-Hydrogen Atoms and Equivalent Isotropic Thermal Parameters for Fe(*t*-BuNC)$_3$(tric) (9b) (Esd's in Parentheses)

atom	x	y	z	U_{eq} (Å^2)[a]	atom	x	y	z	U_{eq} (Å^2)[a]
Fe1[b]	0	0.79327 (15)	0.5	0.0348 (6)	Fe2	0.6645 (2)	0.34793 (15)	0.26372 (8)	0.0394 (7)
O1	0.0137 (10)	1.1123 (9)	0.5145 (3)	0.070 (4)	O8	0.6701 (11)	0.6619 (8)	0.2702 (4)	0.074 (4)
O2	0.1491 (9)	0.9242 (8)	0.3902 (3)	0.068 (4)	O9	0.3309 (8)	0.5526 (9)	0.1824 (3)	0.075 (4)
O3	0.3143 (10)	0.9894 (10)	0.4291 (3)	0.083 (5)	O10	0.2779 (9)	0.4477 (9)	0.2319 (4)	0.087 (5)
O4	0.1982 (8)	0.6008 (9)	0.4456 (3)	0.068 (4)	O11	0.4745 (8)	0.1477 (9)	0.2024 (3)	0.057 (4)
O5	0.3214 (8)	0.7069 (8)	0.4859 (3)	0.069 (4)	O12	0.5037 (9)	0.2773 (9)	0.1555 (3)	0.069 (4)
O6	−0.1156 (9)	1.1356 (8)	0.3975 (3)	0.076 (4)	O13	0.3824 (8)	0.6343 (9)	0.3358 (3)	0.073 (4)
O7	0.0748 (10)	1.1397 (8)	0.4225 (3)	0.074 (4)	O14	0.3877 (12)	0.6715 (10)	0.2689 (4)	0.099 (6)
N1	0.1969 (11)	1.0271 (9)	0.5167 (4)	0.055 (5)	N6	0.6059 (10)	0.5973 (9)	0.2053 (4)	0.057 (5)
N2	0.1384 (9)	0.8035 (9)	0.5459 (3)	0.045 (4)	N7	0.7296 (9)	0.3778 (9)	0.2086 (4)	0.046 (4)
N3	−0.0360 (10)	0.5562 (11)	0.5162 (4)	0.058 (5)	N8	0.7472 (11)	0.1115 (11)	0.2664 (3)	0.053 (5)
N4	−0.2157 (10)	0.7606 (10)	0.4385 (4)	0.061 (5)	N9	0.5700 (11)	0.2784 (10)	0.3427 (4)	0.064 (5)
N5	−0.1734 (11)	0.9156 (11)	0.5477 (4)	0.068 (5)	N10	0.8834 (12)	0.4598 (11)	0.3082 (4)	0.068 (5)
C1	0.0447 (10)	0.9483 (11)	0.4743 (4)	0.041 (5)	C35	0.5572 (12)	0.4959 (11)	0.2600 (4)	0.047 (5)
C2	0.0762 (15)	1.0370 (12)	0.5040 (5)	0.051 (6)	C36	0.6182 (13)	0.5936 (13)	0.2492 (5)	0.056 (7)
C3	0.2456 (11)	0.9212 (11)	0.5043 (5)	0.057 (6)	C37	0.5596 (11)	0.4947 (11)	0.1863 (4)	0.046 (5)
C4	0.1621 (10)	0.8951 (11)	0.4640 (4)	0.044 (5)	C38	0.4882 (12)	0.4480 (11)	0.2206 (4)	0.048 (5)
C5	0.2198 (15)	0.9409 (12)	0.4256 (5)	0.060 (6)	C39	0.3521 (14)	0.4828 (12)	0.2120 (4)	0.051 (6)
C6	0.1911 (14)	0.9781 (15)	0.3545 (5)	0.090 (8)	C40	0.2130 (14)	0.5973 (14)	0.1763 (6)	0.096 (8)
C7	0.1301 (10)	0.7772 (10)	0.4578 (4)	0.039 (4)	C41	0.4992 (12)	0.3250 (9)	0.2287 (5)	0.044 (5)
C8	0.2244 (13)	0.6970 (12)	0.4654 (4)	0.049 (5)	C42	0.4929 (11)	0.2544 (13)	0.1911 (5)	0.050 (6)
C9	0.2919 (15)	0.5156 (12)	0.4519 (6)	0.095 (8)	C43	0.4707 (13)	0.0695 (13)	0.1685 (5)	0.074 (7)
C10	0.2342 (13)	0.8488 (11)	0.5407 (4)	0.047 (5)	C44	0.6706 (13)	0.4268 (11)	0.1788 (5)	0.049 (5)
C11	0.1268 (14)	0.7456 (14)	0.5866 (5)	0.066 (6)	C45	0.8432 (11)	0.3244 (11)	0.1998 (5)	0.056 (6)
C12	0.1364 (17)	0.8277 (16)	0.6216 (5)	0.105 (9)	C46	0.9334 (14)	0.4085 (16)	0.1863 (6)	0.100 (8)
C13	0.2187 (19)	0.6537 (17)	0.5931 (6)	0.117 (10)	C47	0.8215 (15)	0.2317 (14)	0.1690 (5)	0.088 (8)
C14	−0.0490 (11)	0.9886 (11)	0.4396 (4)	0.051 (5)	C48	0.4921 (13)	0.5140 (12)	0.2985 (5)	0.060 (6)
C15	−0.0194 (14)	1.0941 (12)	0.4198 (5)	0.051 (5)	C49	0.4169 (14)	0.6123 (16)	0.2978 (7)	0.079 (8)
C16	−0.0952 (18)	1.2362 (15)	0.3758 (6)	0.113 (9)	C50	0.3150 (15)	0.7326 (14)	0.3394 (7)	0.108 (9)
C17	0.2662 (19)	1.1101 (18)	0.5392 (7)	0.102 (10)	C51	0.6486 (15)	0.6932 (12)	0.1823 (6)	0.080 (7)
C18	0.345 (2)	1.1736 (19)	0.5159 (8)	0.150 (11)	C52	0.543 (2)	0.7453 (16)	0.1559 (7)	0.131 (10)
C19	0.286 (2)	1.098 (2)	0.5826 (8)	0.180 (16)	C53	0.747 (2)	0.6710 (16)	0.1582 (9)	0.169 (16)
C20	−0.0198 (10)	0.6478 (12)	0.5129 (4)	0.036 (5)	C54	0.7184 (10)	0.2026 (13)	0.2638 (4)	0.043 (5)
C21	−0.0428 (18)	0.4347 (15)	0.5189 (7)	0.083 (8)	C55	0.7551 (14)	−0.0058 (11)	0.2665 (5)	0.058 (6)
C22	0.057 (2)	0.389 (2)	0.5015 (12)	0.22 (2)	C56	0.8025 (19)	−0.0445 (15)	0.2279 (7)	0.116 (9)
C23	−0.037 (4)	0.402 (2)	0.5615 (9)	0.27 (3)	C57	0.6356 (16)	−0.0534 (13)	0.2747 (6)	0.091 (8)
C24	−0.151 (3)	0.400 (2)	0.4943 (14)	0.31 (3)	C58	0.8476 (16)	−0.0285 (14)	0.3043 (6)	0.101 (9)
C25	−0.1271 (13)	0.7732 (10)	0.4594 (4)	0.038 (5)	C59	0.6024 (11)	0.3094 (11)	0.3127 (5)	0.045 (5)
C26	−0.3369 (12)	0.7493 (13)	0.4182 (4)	0.060 (6)	C60	0.5162 (15)	0.2403 (14)	0.3790 (5)	0.066 (7)
C27	−0.3740 (16)	0.6293 (14)	0.4185 (6)	0.107 (9)	C61	0.5377 (19)	0.1217 (18)	0.3830 (8)	0.153 (13)
C28	−0.4108 (14)	0.8161 (18)	0.4462 (8)	0.138 (12)	C62	0.567 (2)	0.299 (2)	0.4153 (7)	0.190 (18)
C29	−0.3448 (14)	0.7900 (16)	0.3746 (5)	0.097 (8)	C63	0.3814 (16)	0.269 (2)	0.3735 (6)	0.140 (12)
C30	−0.1067 (12)	0.8624 (10)	0.5316 (3)	0.038 (5)	C64	0.8043 (13)	0.4160 (11)	0.2917 (4)	0.045 (5)
C31	−0.2426 (19)	1.0007 (17)	0.5627 (6)	0.100 (9)	C65	0.9720 (14)	0.5342 (14)	0.3242 (6)	0.071 (7)
C32	−0.172 (3)	1.056 (2)	0.5964 (8)	0.199 (16)	C66	0.975 (2)	0.632 (2)	0.2965 (10)	0.212 (16)
C33	−0.2833 (18)	1.0754 (15)	0.5241 (6)	0.117 (9)	C67	0.947 (3)	0.573 (2)	0.3623 (11)	0.223 (19)
C34	−0.353 (2)	0.9530 (18)	0.5776 (8)	0.173 (14)	C68	1.0925 (16)	0.4789 (18)	0.3321 (9)	0.156 (13)
					Cl1	0.6762 (5)	0.6415 (6)	0.55301 (19)	0.132 (3)
					Cl2	0.4967 (7)	0.4765 (6)	0.5584 (3)	0.168 (3)
					C90	0.5271 (15)	0.6127 (17)	0.5580 (7)	0.124 (10)

[a] $U_{eq} = {}^1/_3\sum_i\sum_j U_{ij}a_i^*a_j^*\mathbf{a}_i\mathbf{a}_j$. [b] Fixed.

metallic complex **9**, in which two coupled alkenes are bound to the metal and the DAB ligand in a tricyclic complex, and the organic dimeric product tetramethyl 2-butene-1,2,3,4-tetracarboxylate (**8**, TMBC), resulting from the coupling of two alkenes. The synthesis of the organic dimer **8** via an electrochemical route has already been described by Kern and Schäfer.[26] The product distribution of **8**:**9** is temperature-dependent. At low temperatures (243 K) mainly the organometallic complex **9** is produced, and at higher temperatures (273 K) the organic dimer **8** is formed.

Molecular Structure of Fe(2,6-xylylNC)$_3$([2.2.2]bic) (7a). The bond lengths and bond angles of the bicyclic complex **7a** are given in Tables V and VI. The molecular structure together with the atomic numbering is given in Figure 1. The structure consists of a [2.2.2] bicyclic structure, in which the bridgehead positions are occupied by the former imine carbon atom and the central metal atom. The geometry around the iron atom resembles a slightly distorted octahedron. The trans positions of the octahedron are occupied by the inserted isocyanide carbon atom C1 and the isocyanide carbon atom C17, by the former alkene carbon atom C4 and the terminal CNR atom C18, and by the isocyanide atom C16 and the imine nitrogen atom N2. The influence of the different atoms in trans positions results in characteristic variations of the bond lengths of the isocyanides to iron. In comparison to the bond lengths of Fe–C17 and Fe–C18 (1.864 (4) and 1.825 (4) Å, respectively) the bond length of Fe–C16 (1.805 (3) Å) is somewhat shortened, due to the good donor N2 in a trans position. The plane formed by Fe–C1–C2–N1 makes an angle of 127.1° with the Fe–C2–C5–N2 plane. The two planes form angles of 117.0 and 115.9°, respectively, with respect to the Fe–C2–C3–C4 plane. The central bond of the former alkene (C3–C4) has been reduced to a single bond, which is reflected in a bond length of 1.543 (5) Å. The hybridization of the two carbon atoms has changed from sp^2 to sp^3, resulting in an average

(26) Kern, J. M.; Schäfer, H. J. *Electrochim. Acta* **1985**, *30*, 81.

Scheme II. Reaction of Fe(CNR)$_3$(*i*-Pr-DAB) (6a–c) with DMM

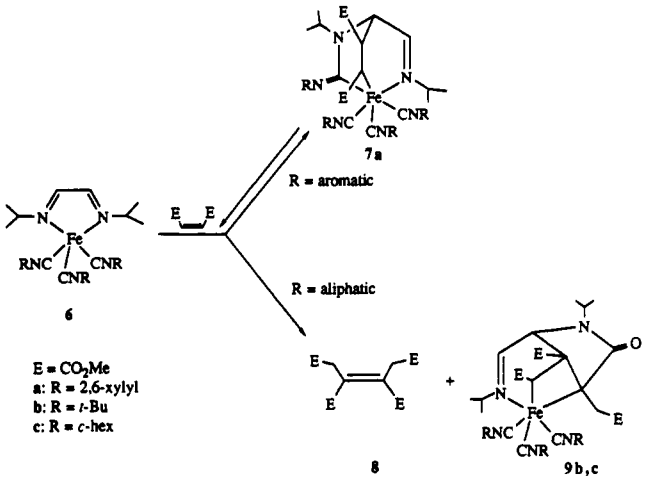

Table V. Bond Distances (Å) for the Non-Hydrogen Atoms of Fe(2,6-xylylNC)$_3$([2.2.2]bic) (7a) (Esd's in Parentheses)

Fe–C1	2.004 (4)	Fe–C4	2.159 (4)	Fe–C16	1.805 (3)
Fe–C17	1.864 (4)	Fe–C18	1.825 (4)	Fe–N2	1.991 (3)
C1–N1	1.338 (5)	C1–N3	1.301 (5)	C2–C3	1.540 (6)
C2–C5	1.482 (6)	C2–N1	1.468 (5)	C3–C4	1.543 (5)
C3–C12	1.500 (6)	C4–C14	1.447 (6)	C5–N2	1.270 (5)
C6–C7	1.527 (8)	C6–C8	1.524 (8)	C6–N1	1.488 (5)
C9–C10	1.512 (8)	C9–C11	1.520 (7)	C9–N2	1.506 (5)
C12–O1	1.215 (6)	C12–O2	1.349 (6)	C13–O2	1.461 (6)
C14–O3	1.217 (5)	C14–O4	1.370 (5)	C15–O4	1.447 (6)
C16–N4	1.162 (5)	C17–N5	1.176 (5)	C18–N6	1.172 (6)
C31–C32	1.407 (6)	C31–C36	1.400 (6)	C31–N3	1.397 (5)
C32–C33	1.398 (7)	C32–C37	1.518 (9)	C33–C34	1.376 (8)
C34–C35	1.380 (8)	C35–C36	1.389 (7)	C36–C38	1.512 (7)
C41–C42	1.393 (7)	C41–C46	1.384 (6)	C41–N4	1.402 (5)
C42–C43	1.398 (6)	C42–C47	1.503 (8)	C43–C44	1.363 (9)
C44–C45	1.373 (9)	C45–C46	1.401 (7)	C46–C48	1.505 (8)
C51–C52	1.384 (6)	C51–C56	1.383 (6)	C51–N5	1.397 (5)
C52–C53	1.396 (7)	C52–C57	1.501 (7)	C53–C54	1.369 (8)
C54–C5	1.365 (9)	C55–C56	1.392 (7)	C56–C58	1.494 (8)
C61–C62	1.392 (7)	C61–C66	1.399 (6)	C61–N6	1.402 (6)
C62–C63	1.406 (8)	C62–C67	1.488 (8)	C63–C64	1.353 (9)
C64–C65	1.37 (1)	C65–C66	1.387 (8)	C66–C68	1.502 (8)

bond angle of 109.3°. The cis position of the two ester functions in the starting alkene is maintained in the organometallic complex, indicating a concerted process for the cycloaddition step (vide infra). The torsion angle between the two ester groups amounts to only 17°. As a result of the insertion the C1–N3 bond length has been elongated to 1.301 (5) Å. The bond angle at N3 has changed from linear to 132.5 (3)°.

The C≡N and the N—C bond lengths of the terminal isocyanides are 1.17 Å (mean) and 1.40 Å (mean), respectively, clearly indicating a triple and a single bond. The bond angles around the three isocyanide nitrogen atoms N4, N5, and N6 are 178.7 (4), 165.4 (4), and 171.9 (4)°, respectively, i.e., close to linear. These bond lengths and bond angles are commonly observed for terminal isocyanides.[10,11]

Molecular Structure of TMBC (8). The bond lengths and angles are presented in Tables VII and VIII. Figure 2 shows the molecular structure together with the atomic numbering. The two original alkene units in the dimeric structure are clearly visible. As a result of the coupling, the former double bond (C1–C4) has been reduced to a single bond (1.504 (3) Å). Also, the hybridization of atom C4 has changed from sp^2 to sp^3, reflected by its tetrahedral bond angle of 109.3°. The two alkenes are connected by a double bond, C1–C1* (1.344 (3) Å). The two ester functions on the new double bond are in a cis position.

Molecular Structure of Fe(*t*-BuNC)$_3$(tric) (9b). The asymmetric unit of the unit cell contains two independent molecules of **9b**, a CH_2Cl_2 solvate molecule, and a disordered Et_2O solvate molecule. Since the **9b** molecules only differ in rotations of the ester group C5-(O3)O2C6 around the C4–C5 axis and of two terminal isocyanides around the terminal C≡N axis, only one structure will be discussed. In Tables IX and X the bond distances and angles are given. The molecular structure and the atomic numbering are presented in Figure 3. The rather exotic molecular structure of the tricyclic complex is composed of a six- (C7–C4–C3–C10–N2–Fe), a five- (C1–C2–N1–C3–C4), and a four-membered ring (C1–C4–C7–Fe). The geometry around the central iron atom resembles a distorted octahedron. The two former alkene bonds (C7–C4 and C1–C14) are lengthened to 1.496 (18) and 1.521 (18) Å, respectively, clearly indicating a change from a double to a single bond. The former alkene with carbon atoms C1 and C14 has undergone the greatest changes. The methoxy group of the ester unit bonded to C1 is removed, while the carboxy group is incorporated in the five-membered γ-lactam ring. The former alkene carbon atom C14 has obtained an extra proton and is not incorporated in one of the three rings.

The bond lengths and angles of the three terminal isocyanides are in accordance with those encountered in many other terminal isocyanide containing complexes.[10,11]

NMR Spectroscopy. ^{1}H NMR and ^{13}C NMR data for Fe(2,6-xylylNC)$_3$([2.2.2]bic) (**7a**), TMBC (**8**), and Fe(CNR)$_3$(tric) (**9b,c**) are listed in Tables XI and XII.

^{1}H NMR. As a result of the cycloaddition reaction, one of the imine carbon atoms (C2) of the DAB ligand in Fe(2,6-xylylNC)$_3$([2.2.2]bic) (**7a**) has been rehybridized from sp^2 to sp^3. Consequently, the proton of the former imine carbon atom has shifted ca. 4 ppm upfield compared to the remaining imine proton. Besides a coupling with the intact imine proton (5 Hz) the amine proton also couples with the former alkene proton (3 Hz), resulting in a double doublet at 4.58 ppm. The former alkene protons at C3 and C4 have very similar chemical shifts, resulting in an AB signal centered at 3.19 ppm. It is partially covered by the signal of one of the ester methyl groups, which show a greater shift difference (3.65 and 3.29 ppm). The inserted 2,6-xylyl isocyanide has lost a rotational degree of freedom around the axis N3–C31–C34, rendering the halves of the aryl ring inequivalent. The two methyl groups are visible as two separate singlets at 2.05 and 1.89 ppm. Likewise, the two meta protons are split into two doublets (7 Hz) at 6.71 and 6.62 ppm. The para proton gives rise to a pseudotriplet at 6.35 ppm (7 Hz). In comparison to the bulk of the signals of the aromatic protons of the terminal isocyanides at 7.20–6.90 ppm, the aromatic protons of the inserted isocyanide are shifted upfield.

The high degree of symmetry of the dimeric compound TMBC (**8**) is clearly visible from its straightforward spectrum. The two sets of inequivalent ester methyl groups give rise to two singlets at 3.79 and 3.70 ppm. The methylene groups resonate as a singlet at 3.48 ppm.

In Fe(CNR)$_3$(tric) (**9b,c**), the two imine units of the former DAB ligand have become inequivalent. The former imine carbon atom C3 has been rehybridized from sp^2 to sp^3, resulting in an upfield shift of ca. 3 ppm of the former imine proton to 5.12 ppm. The three inequivalent ester

Table VI. Bond Angles (deg) for the Non-Hydrogen Atoms of Fe(2,6-xylylNC)$_3$([2.2.2]bic) (7a) (Esd's in Parentheses)

C1–Fe–C4	88.0 (2)	C1–Fe–C16	86.2 (2)	C1–Fe–C17	174.0 (2)
C1–Fe–C18	85.1 (2)	C1–Fe–N2	90.8 (1)	C4–Fe–C16	86.2 (2)
C4–Fe–C17	95.4 (2)	C4–Fe–C18	173.1 (2)	C4–Fe–N2	86.5 (1)
C16–Fe–C17	89.1 (2)	C16–Fe–C18	92.7 (2)	C16–Fe–N2	172.2 (2)
C17–Fe–C18	91.4 (2)	C17–Fe–N2	94.3 (1)	C18–Fe–N2	94.2 (1)
Fe–C1–N1	118.2 (3)	Fe–C1–N3	119.0 (3)	N1–C1–N3	122.8 (3)
C3–C2–C5	110.3 (3)	C3–C2–N1	110.1 (3)	C5–C2–N1	112.7 (4)
C2–C3–C4	114.0 (3)	C2–C3–C12	109.6 (3)	C4–C3–C12	114.3 (3)
Fe–C4–C3	111.7 (3)	Fe–C4–C14	105.9 (3)	C3–C4–C14	113.4 (3)
C2–C5–N2	120.2 (3)	C7–C6–C8	112.1 (4)	C7–C6–N1	110.6 (4)
C8–C6–N1	111.7 (4)	C10–C9–C11	111.5 (4)	C10–C9–N2	110.1 (4)
C11–C9–N2	112.4 (4)	C3–C12–O1	126.2 (5)	C3–C12–O2	110.7 (4)
O1–C12–O2	123.0 (4)	C4–C14–O3	127.1 (4)	C4–C14–O4	112.7 (3)
O3–C14–O4	120.1 (4)	Fe–C16–N4	176.6 (4)	Fe–C17–N5	173.1 (3)
Fe–C18–N6	177.4 (3)	C32–C31–C36	119.0 (4)	C32–C31–N3	121.2 (4)
C36–C31–N3	118.7 (4)	C31–C32–C33	119.1 (5)	C31–C32–C37	120.2 (4)
C33–C32–C37	120.7 (5)	C32–C33–C34	121.5 (5)	C33–C34–C35	119.3 (5)
C34–C35–C36	120.8 (5)	C31–C36–C35	120.3 (4)	C31–C36–C38	119.4 (4)
C35–C36–C38	120.3 (4)	C42–C41–C46	123.7 (4)	C42–C41–N4	117.4 (4)
C46–C41–N4	118.9 (4)	C41–C42–C43	117.2 (5)	C41–C42–C47	121.8 (4)
C43–C42–C47	121.0 (5)	C42–C43–C44	119.9 (5)	C43–C44–C45	122.1 (5)
C44–C45–C46	120.2 (5)	C41–C46–C45	116.8 (5)	C41–C46–C48	121.8 (4)
C45–C46–C48	121.4 (5)	C52–C51–C56	123.2 (4)	C52–C51–N5	118.3 (3)
C56–C51–N5	118.5 (4)	C51–C52–C53	117.6 (4)	C51–C52–C57	120.7 (4)
C53–C52–C57	121.7 (4)	C52–C53–C54	119.9 (5)	C53–C54–C55	121.4 (5)
C54–C55–C56	120.7 (5)	C51–C56–C55	117.1 (4)	C51–C56–C58	122.1 (4)
C55–C56–C58	120.8 (4)	C62–C61–C66	123.2 (4)	C62–C61–N6	119.6 (4)
C66–C61–N6	117.1 (4)	C61–C62–C63	116.8 (5)	C61–C62–C67	121.7 (5)
C63–C62–C67	121.4 (5)	C62–C63–C64	120.3 (6)	C63–C64–C65	122.2 (6)
C64–C65–C66	120.4 (5)	C61–C66–C65	117.0 (5)	C61–C66–C68	121.3 (4)
C65–C66–C68	121.6 (5)	C1–N1–C2	116.7 (3)	C1–N1–C6	122.1 (3)
C2–N1–C6	116.8 (3)	Fe–N2–C5	119.8 (3)	Fe–N2–C9	122.6 (2)
C5–N2–C9	117.6 (3)	C1–N3–C31	132.5 (3)	C16–N4–C41	178.7 (4)
C17–N5–C51	171.9 (4)	C18–N6–C61	165.4 (4)	C12–O2–C13	115.5 (4)
C14–O4–C15	115.8 (3)				

methyl groups appear as three separate singlets. The proton on the former alkene carbon atom (C7), directly bonded to the metal, gives a singlet near 2.30 ppm. The two diastereotopic protons of the methylene group (C14) give rise to two doublets ($^2J_{HH}$ = 18 Hz) at 3.19 and 3.12 ppm. The three terminal isocyanides give rise to three separate sets of signals: while the *t*-Bu groups of complex **9b** give three singlets, for complex **9c** with cyclohexyl isocyanide this results in a complex pattern of multiplets.

^{13}C NMR. The remaining imine carbon nucleus (C5) of Fe(2,6-xylylNC)$_3$([2.2.2]bic) (**7a**) resonates at 170.5 ppm, whereas the C–C-coupled former imine carbon (C2) gives rise to a signal at 55.2 ppm. The upfield shift reflects the change in hybridization from sp^2 to sp^3. The former alkene carbon atom (C3), bonded to the DAB ligand, resonates at 51.0 ppm, and the other former alkene carbon atom (C4), σ-bonded to the iron, resonates at 23.1 ppm. The assignment is based on HETCOR (^{13}C,^{1}H) measurements. The rotational fixation of the inserted isocyanide is also reflected in the ^{13}C NMR spectrum, as shown by the two signals at 19.5 and 18.3 ppm for the two inequivalent methyl groups (C37, C38). The terminal isocyanide carbon nuclei give rise to three separate signals around 183 ppm, and also the six methyl groups give three signals around 19 ppm. These data indicate that the three terminal isocyanide ligands do not interchange positions on the NMR time scale but that the aryl rings can rotate freely.

The ^{13}C NMR spectrum of TMBC (**8**) and the assignments in Table XII are as straightforward as the proton spectrum. Only one of the identical halves of the molecule is indicated. The resonances of the two inequivalent carboxy atoms C2 and C5 cannot be individually assigned.

The remaining imine carbon nuclei in the two Fe(CNR)$_3$(tric) complexes **9b,c** resonate at 167.5 and 168.6 ppm. The three carboxy atoms of the ester groups and the carboxy atom of the lactam ring resonate at around 178 ppm. The two carbon nuclei σ-bonded to the metal are found at 7 and 20 ppm. A comparable high-field shift, due to the diamagnetic shielding of the iron atom, is also encountered for the σ-bonded carbon atom in the bicyclic compound **7a**. The three terminal isocyanide carbon nuclei give rise to three separate signals near 172 ppm, indicating that the isocyanides do not interchange positions on the NMR time scale.

IR Spectroscopy. The IR data for Fe(2,6-xylylNC)$_3$([2.2.2]bic) (**7a**), TMBC (**8**), and Fe(CNR)$_3$(tric) (**9b,c**) together with the elemental analyses are listed in Table XIII. The IR spectra of the organometallic complexes show three intense absorptions in the characteristic $\nu_{C\equiv N}$ region. The C≡N stretching bands of the bicyclic complex **7a** are found at frequencies significantly lower than those of the tricyclic compounds **9b,c**. This is ascribed to the type of isocyano group, i.e., aliphatic in **9b,c** and aromatic in **7a**. The better electron-withdrawing properties of the aryl group reduces the C–N bond order and consequently the stretching frequency.[10,11b,27]

Discussion

The product distribution depends on the type of R group of the isocyanide, i.e., aliphatic or aromatic. Since the

(27) (a) Saillard, J. Y.; Le Beuze, A.; Simmoneaux, G.; Le Maux, P.; Jaouen, G. *J. Mol. Struct.* **1981**, *86*, 149. (b) Dickson, C. A.; McFarlaine, A. W.; Coville, N. J. *Inorg. Chim. Acta* **1989**, *158*, 205. (c) Minelli, M.; Maley, W. J. *Inorg. Chem.* **1989**, *20*, 2954. (d) Fantucci, P.; Naldini, L.; Cariati, F.; Valenti, V. *J. Organomet. Chem.* **1974**, *64*, 190. (e) Malatesta, L.; Bonati, F. In *Isocyanide Complexes of Metals*; Wiley: New York, 1969; p 7. (f) de Lange, P. P. M.; Kraakman, M. J. A.; van Wijnkoop, M.; Frühauf, H.-W.; Vrieze, K.; Smeets, W. J. J.; Spek, A. L. *Inorg. Chim. Acta* **1992**, *196*, 151. (g) Vaughan, L. G.; Sheppard, W. A. *J. Am. Chem. Soc.* **1969**, *91*, 6151. (h) Harvey, P. D.; Butler, I. S.; Barreto, M. de C.; Coville, N. J.; Harris, G. W. *Inorg. Chem.* **1988**, *27*, 639. (i) *Isonitrile Chemistry*; *Organic* Chemistry 20; Ugi, I., Ed.; Academic Press: New York, London, 1971; p 221.

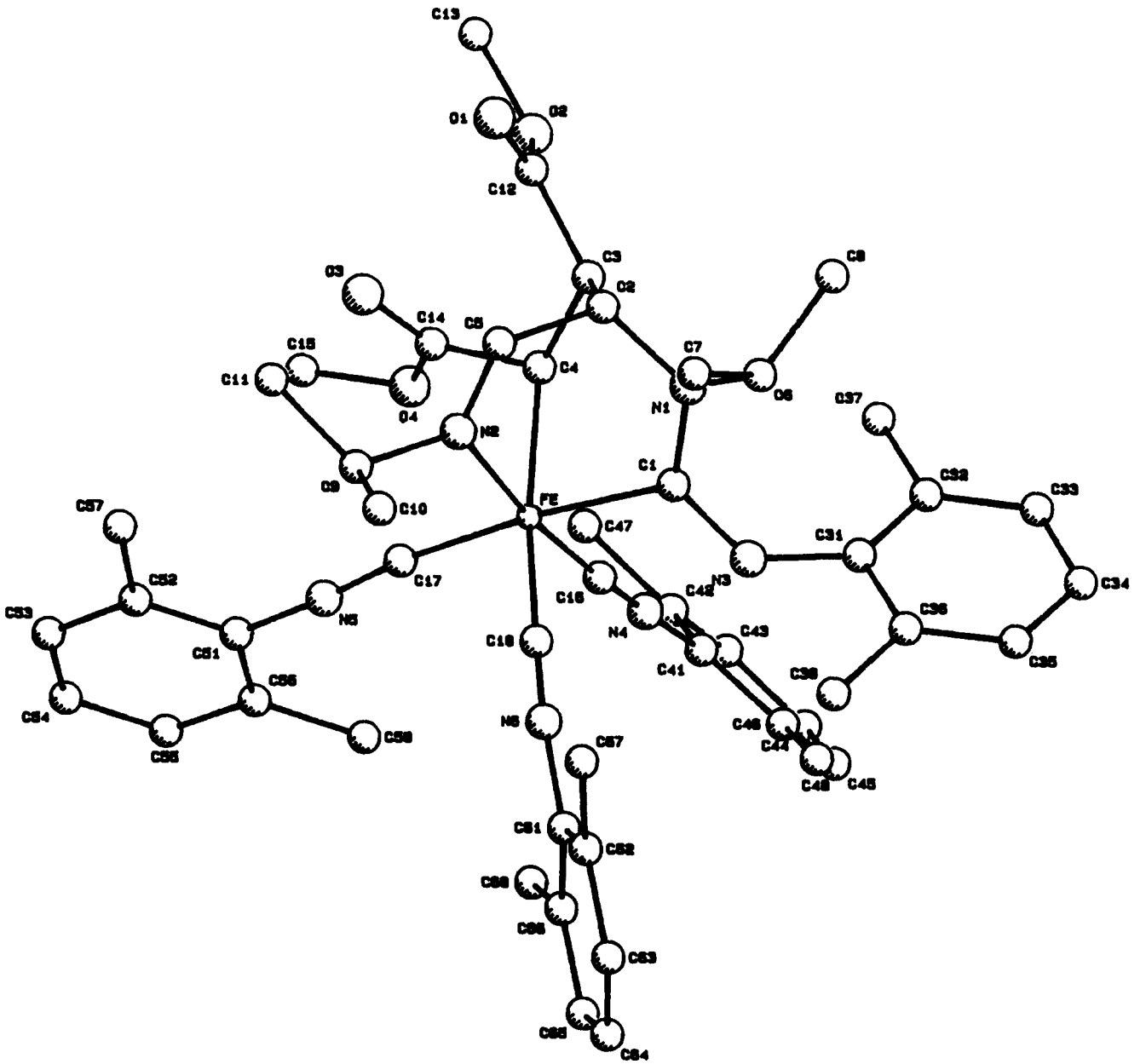

Figure 1. PLUTO drawing of Fe(2,6-xylylNC)$_3$([2.2.2]bic (7a). Hydrogen atoms were left out for clarity.

Table VII. Bond Distances (Å) for the Non-Hydrogen Atoms of TMBC (8) (Esd's in Parentheses)

C1–C1*	1.344 (3)	C1–C2	1.499 93)
C1–C4	1.504 (3)	C2–O1	1.199 (3)
C2–O2	1.329 (3)	C3–O2	1.451 (4)
C4–C5	1.505 (3)	C5–O3	1.200 (3)
C5–O4	1.327 (3)	C6–O4	1.455 (5)

Table VIII. Bond Angles (deg) for the Non-Hydrogen Atoms of TMBC (8) (Esd's in Parentheses)

C1*–C1–C2	120.4 (2)	C1*–C1–C4	125.4 (2)
C2–C1–C4	114.1 (2)	C1–C2–O1	122.7 (2)
C1–C2–O2	113.0 (2)	O1–C2–O2	124.3 (2)
C1–C4–C5	111.8 (2)	C4–C5–O3	124.4 (2)
C4–C5–O4	110.8 (2)	O3–C5–O4	124.7 (2)
C2–O2–C3	115.3 (2)	C5–O4–C6	115.2 (3)

types of products that are formed and the reaction mechanisms differ remarkably, the reactions of **6a** (with 2,6-xylyl isocyanide) and of **6b,c** (with the *tert*-butyl (**b**) and cyclohexyl (**c**) isocyanides) will be discussed separately.

Formation of Fe(2,6-xylylNC)$_3$([2.2.2]bic) (7a). As we have described before,[1b,8e,9b] the Fe—N=C fragment in the starting Fe(CNR)$_3$(*i*-Pr-DAB) (**6**) represents an isolobal analogue of an azomethyne ylide ($R_2C{=}N^+C^-R_2$), a classical 1,3-dipole. On this basis, the first step in the reaction sequence (cf. Scheme III) can be looked upon as a [3 + 2] oxidative cycloaddition of DMM across the 1,3-dipolar Fe—N=C fragment, leading to the [2.2.1] bicyclic intermediate **10**, which, however, cannot be observed in the present case. In other comparable systems,[8e,28] this initial cycloadduct could be fully characterized by spectroscopic and X-ray methods. Intermediate **10** then immediately undergoes an insertion reaction leading to the [2.2.2] bicyclic structure **11**. The insertion reaction, proceeding via a nucleophilic attack of the nitrogen lone pair on the terminal carbon atom of an isocyanide ligand, relieves the strain in the one-atom nitrogen bridge. The coordinatively and electronically unsaturated intermediate **11** then readily accepts an extra isocyanide to give the stable [2.2.2] bicyclic complex **7a**.

In the cases of Fe(CO)$_3$(DAB)[8a–e] and monosubstituted Fe(CO)$_2$(CNR)(DAB)[9b] complexes cycloaddition reactions

(28) van Wijnkoop, M.; Vlug, T.; de Lange, P. P. M.; H.-W. Frühauf. To be submitted for publication.

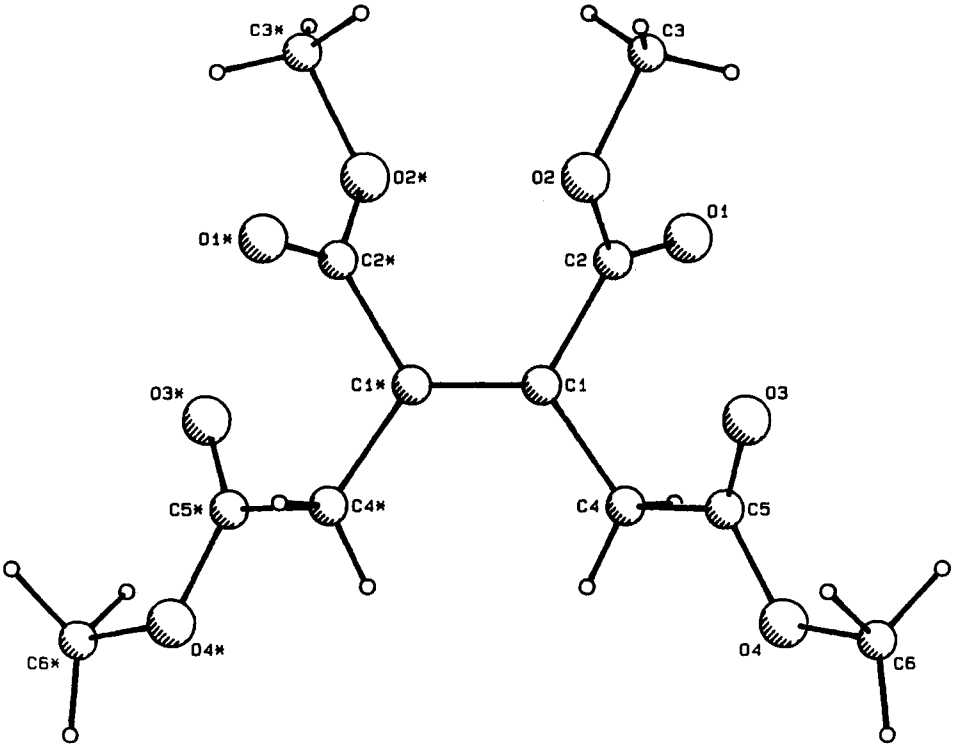

Figure 2. PLUTO drawing of TMBC (8).

Table IX. Bond Distances (Å) for the Non-Hydrogen Atoms of Fe(*t*-BuNC)$_3$(tric) (9b) (Esd's in Parentheses)

Fe–N2	2.017 (10)	Fe–C1	2.152 (13)	Fe–C7	2.105 (12)
Fe–C20	1.848 (15)	Fe–C25	1.834 (14)	Fe–C30	1.855 (12)
O1–C2	1.228 (19)	O2–C5	1.324 (19)	O2–C6	1.444 (19)
O3–C5	1.21 (2)	O4–C8	1.355 (18)	O4–C9	1.478 (19)
O5–C8	1.211 (17)	O6–C15	1.326 (19)	O6–C16	1.45 (2)
O7–C15	1.188 (19)	N1–C2	1.37 (2)	N1–C3	1.479 (18)
N1–C17	1.42 (2)	N2–C10	1.236 (18)	N2–C11	1.502 (19)
N3–C20	1.14 (2)	N3–C21	1.49 (2)	N4–C25	1.144 (18)
N4–C26	1.445 (18)	N5–C30	1.155 (18)	N5–C31	1.41 (2)
C1–C2	1.46 (2)	C1–C4	1.535 (17)	C1–C14	1.521 (18)
C3–C4	1.540 (19)	C3–C10	1.48 (2)	C4–C5	1.56 (2)
C4–C7	1.496 (18)	C7–C8	1.443 (19)	C11–C12	1.50 (2)
C11–C13	1.52 (3)	C14–C15	1.49 (2)	C17–C18	1.45 (3)
C17–C19	1.39 (3)	C21–C22	1.42 (3)	C21–C23	1.42 (4)
C21–C24	1.43 (4)	C26–C27	1.53 (2)	C26–C28	1.52 (3)
C26–C29	1.48 (2)	C31–C32	1.43 (3)	C31–C33	1.56 (3)
C31–C34	1.49 (3)				

were only possible with alkynes bearing electron-withdrawing substituents. This clearly points to a type of cycloaddition reaction with a nucleophilic or HOMO-controlled 1,3-dipole, according to the Sustmann classification.[29] This implies a reaction in which the interactions of the HOMO of the dipole and the LUMO of the dipolarophile dominate. Also, calculations for the isolobal analogue of the Fe—N=C unit, azomethyne ylides, clearly revealed that they are electron-rich species with comparatively high HOMO and LUMO levels.[30] Preliminary CAS-SCF calculations comparing the two systems indeed point to high-lying HOMO and LUMO levels.[31] Cycloaddition reactions with a nucleophilic dipole are promoted by electron-donating substituents on the 1,3-dipole. This substitution will raise the dipole HOMO level, resulting in an enhanced frontier orbital overlap. Consequently, the introduction of three better σ-donating/worse π-accepting[10,11] isocyanide ligands results in a higher 1,3-dipolar activity of the metal DAB fragment compared to that in the CO-containing complexes.[1b] This enhanced activity allows for the observed cycloaddition reaction with the less activated alkene[30b] as dipolarophile.

The [2.2.2] bicyclic compound **3**, formed in the reactions of Fe(CO)$_3$(DAB) with alkynes (see Scheme I), isomerized on warming via reductive elimination followed by recoordination of the double bond to give the stable Fe(CO)$_3$(1,5-dihydropyrrol-2-one) complex **4**. The present [2.2.2] tris(isocyanide) bicyclic compound **7a**, lacking the double bond in the two-carbon bridge, is found to behave differently. The yellow iron complex **7a** is stable as a solid, but in solution it is easily converted back to the starting compounds when the solution is warmed above room temperature (Scheme III). The process is accompanied by a spectacular color change from yellow to deep dark red, indicative of the existence of the chelating α-diimine complex **6a**. The reaction already proceeds, although more slowly (completion after ca. 5 h), at 303 K,[32] while at 333 K the reaction time is ca. 1.5 h. When the mixture was cooled to room temperature, the yellow [2.2.2] bicyclic complex **7a** was slowly formed back in about 1 day. At still lower temperatures, the equilibrium between the starting compounds and the [2.2.2] bicyclic complex **7a** is frozen in. The assembly and disassembly of **7a** can be followed by NMR (vide infra) for only a limited number

(29) (a) Sustmann, R. *Tetrahedron Lett.* **1971**, 2721. (b) Sustmann, R.; Trill, H. *Angew. Chem., Int. Ed. Engl.* **1972**, *11*, 838. (c) Sustmann, R. *Pure Appl. Chem.* **1974**, *40*, 569. (d) Fukui, K. *Acc. Chem. Res.* **1971**, *4*, 57. (e) Herndon, W. C. *Chem. Rev.* **1972**, *72*, 157. (f) Houk, K. N.; Yamaguchi, K. In *1,3-Dipolar Cycloaddition Chemistry*; Padwa A., Ed.; Wiley: New York, 1984; Chapter 13. (g) Bastide, J.; El Ghandour, N.; Henri-Rousseau, O. *Tetrahedron Lett.* **1972**, *41*, 4225.

(30) (a) Houk, K. N. *Acc. Chem. Res.* **1975**, *8*, 361. (b) Houk, K. N.; Sims, J.; Duke, R. E.; Strozier, R. W.; George, J. K. *J. Am. Chem. Soc.* **1973**, *95*, 7287. (c) Lown, J. W. In *1,3-Dipolar Cycloaddition Chemistry*; Padwa, A., Ed.; Wiley: New York, 1984; Chapter 6.

(31) Dedieu, A.; Liddell, M. J. To be submitted for publication.

(32) The [2.2.2] bicyclic complex **7a** is synthesized at lower temperatures. This apparent contradiction can be explained by noticing that the polar complex **7a** is insoluble in, and therefore is immediately precipitated from, the pentane solution; i.e., even a very small equilibrium concentration of **7a** at low temperature is precipitated and the equilibrium is shifted toward product **7a**.

Table X. Bond Angles (deg) for the Non-Hydrogen Atoms of Fe(*t*-BuNC)$_3$(tric) (9b) (Esd's in Parentheses)

N2–Fe–C1	91.8 (4)	N2–Fe–C7	86.7 (4)	N2–Fe–C20	89.9 (5)
N2–Fe–C25	175.7 (5)	N2–Fe–C30	93.7 (5)	C1–Fe–C7	68.2 (5)
C1–Fe–C20	167.3 (5)	C1–Fe–C25	92.4 (5)	C1–Fe–C30	89.9 (5)
C7–Fe–C20	99.3 (5)	C7–Fe–C25	94.1 (5)	C7–Fe–C30	158.1 (5)
C20–Fe–C25	85.8 (5)	C20–Fe–C30	102.6 (5)	C25–Fe–C30	87.2 (5)
C5–O2–C6	113.0 (12)	C8–O4–C9	115.9 (11)	C15–O6–C16	115.0 (12)
C2–N1–C3	112.2 (11)	C2–N1–C17	123.3 (14)	C3–N1–C17	124.4 (13)
Fe–N2–C10	122.5 (9)	Fe–N2–C11	118.0 (8)	C10–N2–C11	119.3 (11)
C20–N3–C21	173.2 (14)	C25–N4–C26	170.5 (14)	C30–N5–C31	166.7 (16)
Fe–C1–C2	117.0 (9)	Fe–C1–C4	87.1 (8)	Fe–C1–C14	113.3 (8)
C2–C1–C4	107.7 (11)	C2–C1–C14	109.3 (11)	C4–C1–C14	121.4 (11)
O1–C2–N1	123.9 (14)	O1–C2–C1	129.3 (15)	N1–C2–C1	106.6 (12)
N1–C3–C4	101.5 (10)	N1–C3–C10	104.3 (12)	C4–C3–C10	115.9 (11)
C1–C4–C3	100.8 (10)	C1–C4–C5	117.2 (11)	C1–C4–C7	103.9 (10)
C3–C4–C5	108.7 (11)	C3–C4–C7	115.2 (11)	C5–C4–C7	111.0 (11)
O2–C5–O3	126.1 (14)	O2–C5–C4	111.0 (13)	O3–C5–C4	122.8 (13)
Fe–C7–C4	89.8 (7)	Fe–C7–C8	120.1 (9)	C4–C7–C8	118.4 (11)
O4–C8–O5	118.4 (13)	O4–C8–C7	113.4 (11)	O5–C8–C7	128.2 (13)
N2–C10–C3	121.8 (12)	N2–C11–C12	109.0 (13)	N2–C11–C13	110.2 (13)
C12–C11–C13	113.7 (14)	C1–C14–C15	115.0 (11)	O6–C15–O7	121.4 (14)
O6–C15–C14	110.8 (12)	O7–C15–C14	127.8 (14)	N1–C17–C18	116.9 (19)
N1–C17–C19	116.5 (19)	C18–C17–C19	122 (2)	Fe–C20–N3	172.3 (12)
N3–C21–C22	108.8 (17)	N3–C21–C23	109.9 (17)	N3–C21–C24	108.0 (17)
C22–C21–C23	108 (3)	C22–C21–C24	109 (2)	C23–C21–C24	113 (2)
Fe–C25–N4	170.7 (13)	N4–C26–C27	109.4 (13)	N4–C26–C28	103.2 (12)
N4–C26–C29	110.3 (12)	C27–C26–C28	110.3 (13)	C27–C26–C29	110.1 (13)
C28–C26–C29	113.3 (15)	Fe–C30–N5	171.6 (11)	N5–C31–C32	109.1 (19)
N5–C31–C33	106.6 (15)	N5–C31–C34	109.0 (17)	C32–C31–C33	113.9 (18)
C32–C31–C34	111 (2)	C33–C31–C34	107.6 (17)		

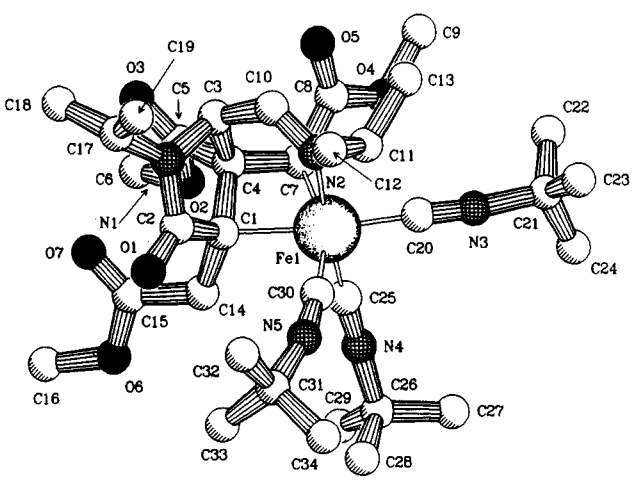

Figure 3. PLUTON drawing of the molecular structure of Fe(*t*-BuNC)$_3$(tric) (**9b**), with the adopted atom labeling. Only one of the two nearly identical molecules in the unit cell is shown. Hydrogen atoms were left out for clarity.

of cycles. Decomposition products, probably due to the very limited stability of starting complex **6a**, then begin to obscure the NMR spectra.

The available evidence indicates microscopic reversibility for the assembly and the disassembly reactions of **7a**, i.e., for the cycle **6a** → [**10** → **11**] → **7a** → [**11** → **10**] → **6a**. When a solution of **7a** is warmed in the presence of excess isocyanide, the disassembly reaction is considerably slowed down; i.e., **7a** is strongly stabilized when the initial dissociative loss of a terminal isocyanide ligand is inhibited. Another indication of the microscopic reversibility is the stereospecificity with respect to the cis configuration of the two ester groups. The molecular structure of the bicyclic complex **7a** (vide supra) already showed the cis relation of the ester groups. When the bicyclic complex is disassembled into its components, the alkene also retains its cis configuration. The retention of configuration in either direction also establishes the concertedness of the 1,3-dipolar cycloaddition and cycloreversion steps.[33]

As has been indicated above, the total reaction cycle has been monitored by variable-temperature ^{1}H NMR in C_6D_6 solution. Figure 4 shows three spectra taken during the disassembly of **7a** into the starting components. Spectrum A shows the pure [2.2.2] bicyclic complex **7a** at 293 K. After the temperature is raised to 333 K, the signals[34] corresponding to Fe(2,6-xylylNC)$_3$(*i*-Pr-DAB), 2,6-xylyl isocyanide, and DMM increase while the signals corresponding to the bicyclic complex decrease. Spectrum C shows the situation when the signals of the bicyclic complex **7a** have nearly vanished, and mainly the signals of the starting compounds are visible. This temperature-controlled molecular self-assembly and -disassembly is unique, considering all the steps involved and because of the ease with which these steps occur. C–C, C–N, and Fe–C σ bonds and an Fe–CNR donative bond are formed and broken during the process. Not many examples are known from the literature where an organic cycloreversion reaction takes place under such mild conditions.[35] Usually an equilibrium in a cycloaddition/cycloreversion reaction is reached at much more elevated temperatures.[36] Cycloreversion reactions of organometallic compounds have very rarely been encountered.[37] An example concerning a retro-Diels–Alder reaction of a dithiin oxide has recently been described by Urove et al.[38]

One of the intriguing aspects of the disassembly reaction

(33) In the analogous reaction of Fe(CO)$_3$(DAB) with alkynes, the polarity of the solvent did not influence the reaction rates or yields.[40a] Therefore, a stepwise mechanism with charge-separated intermediates can be excluded.

(34) ^{1}H NMR data (300.13 MHz, C_6D_6; ppm) of the starting compounds is as follows. (a) Fe(2,6-xylylNC)$_3$(*i*-Pr-DAB) (**6a**): 7.67 (2H, d, 5 Hz; N=C*H*), 6.8–6.6 (9H, m, aryl *H*), 5.39 (2H, sept, 7 Hz, C*H*(CH$_3$)$_2$), 2.35 (18H, s, aryl CH$_3$), 1.68 (12H, d, 7 Hz, CH(CH$_3$)$_2$). (b) 2,6-xylylNC (*a*): 6.8–6.5 (3H, m, aryl *H*), 2.07 (6H, s, aryl CH$_3$). (c) Dimethyl maleate: 5.70 (2H, s, C=C*H*), 3.35 (6H, s, OCH$_3$).

(35) (a) Kaufmann, T. K.; Habersaat, K.; Köppelmann, E. *Chem. Ber.* 1977, *110*, 638. (b) Carrié, R.; Yeung Lam Ko, Y. Y. C.; De Sarlo, F.; Brandi, A. *J. Chem. Soc., Chem. Commun.* 1981, 1131. (c) Bianchi, G.; Gandolfi, R. In *1,3-Dipolar Cycloaddition Chemistry*; Padwa, A., Ed.; Wiley: New York, 1984; Chapter 14.

(36) (a) Wollweber, H. In *Diels-Alder Reaktion*; Georg Thieme Verlag: Stuttgart, Germany, 1972; p 155. (b) Wasserman, A. In *Diels-Alder Reactions*; Elsevier: Amsterdam, 1965; p 61.

Table XI. ^{1}H NMR Data[a] for Fe(2,6-xylylNC)$_3$([2.2.2]bic) (7a), TMBC (8), and Fe(CNR)$_3$(tric) (9b,c)

compd	^{1}H NMR data
7a	8.64 (1 H, d, 5 Hz, *H*C=N), 7.20–6.90 (9 H, m, aryl *H*), 6.71, 6.62 (2 × 1H, 2 × d, 7 Hz, *m* aryl *H*), 6.35 (1H, dd, 7 Hz, 7 Hz, *p* aryl *H*), 4.58 (1H, dd, 5 Hz, 3 Hz, N=CC*H*), 4.36, 4.07 (2 × 1H, 2 × sept, 7 Hz, C*H*(CH$_3$)$_2$), 3.65, 3.29 (2 × 3H, 2 × s, OC*H*$_3$), 3.19 (2H, m, Fe—C*H*—C*H*), 2.39, 2.37, 2.32 (3 × 6H, 3 × s, terminal aryl C*H*$_3$), 2.05, 1.89 (2 × 3H, 2 × s, ring C=N aryl C*H*$_3$), 1.44, 1.33, 0.84, 0.77 (4 × 3H, 4 × d, 7 Hz, CH(C*H*$_3$)$_2$)
7a[b]	8.64 (1H, d, 5 Hz, *H*C=N), 7.01, 6.92 (2 × 1H, 2 × d, 7 Hz, *m* aryl *H*), 6.8–6.66 (9H, m, aryl *H*), 4.72 (1H, dd, 5 Hz, 3 Hz, N=CC*H*), 4.41, 4.21 (2 × 1H, 2 × sept, 7 H, C*H*(CH$_3$)$_2$), 3.60 (2H, m, Fe—C*H*—C*H*), 3.58, 3.41 (2 × 3H, 2 × s, OC*H*$_3$), 2.44, 2.37, 2.36 (3 × 6H, 3 × s, terminal aryl C*H*$_3$), 2.30, 2.19 (2 × 3H, 2 × s, ring C=N aryl C*H*$_3$), 1.48, 1.12, 0.77, 0.72 (4 × 3H, 4 × d, 7 Hz, CH(C*H*$_3$)$_2$)
8	3.48 (2 × 2H, s, C*H*$_2$), 3.70 (2 × 3H, s, OC*H*$_3$), 3.79 (2 × 3H, s, OC*H*$_3$)
9b	8.45 (1H, d, 4 Hz, *H*C=N), 5.12 (1H, d, 4 Hz, N=CC*H*), 4.12 (2H, m, C*H*(CH$_3$)$_2$), 3.49, 3.45, 3.39 (3 × 3H, 3 × s, OC*H*$_3$), 3.19, 3.12 (2 × 1H, 2 × d, 18 Hz, C*H*$_2$), 2.33 (1H, s, Fe—C*H*), 1.54, 1.44, 1.42 (3 × 9H, 3 × s, C≡NC(C*H*$_3$)$_3$), 1.27, 1.20, 1.12 (12H, 3 × d, 7 Hz, CH(C*H*$_3$)$_2$)
9c	8.45 (1H, d, 4 Hz, *H*C=N), 5.11 (1H, d, 4 Hz, N=CC*H*), 4.16 (2H, m, C*H*(CH$_3$)$_2$), 3.85, 3.70 (3H, m, c-Hex C*H*), 3.49, 3.46, 3.38 (3 × 3H, 3 × s, OC*H*$_3$), 3.20, 3.14 (2 × 1H, 2 × d, 18 Hz, C*H*$_2$), 2.36 (1H, s, Fe—C*H*), 1.84–1.10 (42H, m, c-Hex C*H*$_2$, CH(C*H*$_3$)$_2$)

[a] Chemical shifts are in ppm relative to Me$_4$Si, measured in CDCl$_3$ at 293 K and 300.15 MHz. Abbreviations: s = singlet, d = doublet, m = multiplet. [b] Recorded in C$_6$D$_6$.

Table XII. ^{13}C NMR Data[a] for Fe(2,6-xylylNC)$_3$([2.2.2]bic) (7a), TMBC (8), and Fe(CNR)$_3$(tric) (9b,c)

compd	^{13}C NMR data
7a[b]	196.05 (C1), 183.6, 183.0, 182.3 (C16, C17, C18), 176.5, 153.6 (C12, C14), 170.5 (C5), 134.7, 134.3, 134.0 (C42, C46, C62, C66, C52, C56), 129.8, 129.1, 128.7 (C41, C51, C61), 127.7, 127.6, 127.2 (C43, C45, C53, C55, C63, C65), 127.0, 126.6 (C33, C35), 126.6 (C31), 126.3, 126.2, 125.9 (C44, C54, C64), 125.04 (C32, C36), 116.6 (C34), 63.5, 47.0 (C6, C9), 55.2 (C2), 51.0 (C3), 51.5, 49.2 (C13, C15), 24.5, 23.6, 23.3 (C7, C8, C10, C11), 23.1 (C4), 19.5, 18.3 (C37, C38), 19.2, 19.0, 18.9 (C47, C48, C57, C58, C67, C68)
8[c]	169.2, 167.7 (C2, C5), 133.3 (C1), 53.0, 52.7 (C3, C6), 35.3 (C4)
9b[d]	183.0, 180.5, 174.6, 171.6 (C2, C5, C8, C15), 176.4, 168.4, 167.6 (C20, C25, C30), 167.5 (C10), 63.7, 57.2 (C11, C17), 51.0, 50.8, 50.1 (C6, C9, C16), 57.5 (C4), 55.5, 56.1, 56.3 (C21, C26, C31), 42.4 (C3), 41.5 (C14), 31.3, 31.1, 31.0 (C22, C23, C24, C27, C28, C29, C32, C33, C34), 24.3, 23.2, 22.2, 20.6 (C12, C13, C18, C19), 19.2 (C1), 6.5 (C7)
9c[e]	183.5, 172.4, 181.5, 175.3 (C2, C5, C8, C15), 176.3, 170.0, 168.3 (*C*≡N), 168.6 (C10), 64.5, 57.5 (C11, C17), 58.2 (C4), 51.7, 51.6, 50.8 (C6, C9, C16), 42.8, (C3), 42.1 (C14), 32.0, 28.3, 23.4 (c-Hex *C*H), 29.7, 25.9, 25.7, 21.2 (c-Hex *C*H$_2$), 25.1, 24.1, 22.9, 21.5 (C12, C13, C18, C19), 20.1 (C1), 7.9 (C7)

[a] Chemical shifts are in ppm relative to Me$_4$Si, measured in CDCl$_3$ at 243 K and 75.47 MHz. [b] For the atomic numbering see Figure 1. [c] For the atomic numbering see Figure 2. [d] For the atomic numbering see Figure 3. [e] For the atomic numbering of the heterocycle see Figure 3.

Table XIII. IR Data[a] and Elemental Analyses[46] for Fe(2,6-xylylNC)$_3$([2.2.2]bic) (7a), TMBC (8), and Fe(CNR)$_3$(tric) (9b,c)

compd	$\nu_{C\equiv N}$ (cm^{-1})	elemental anal. (%)		
		C_{obs} (C_{calc})	H_{obs} (H_{calc})	N_{obs} (N_{calc})
7a	2120, 2060, 2040	69.43 (69.28)	7.00 (6.95)	9.72 (9.66)
8		49.84 (50.00)	5.56 (5.59)	
9b	2130, 2075, 2060	56.90 (58.20)	7.85 (7.76)	9.75 (9.99)
9c	2130, 2085, 2055	60.08 (61.61)	7.84 (7.89)	8.69 (8.98)

[a] Recorded in CHCl$_3$.

is the ready isocyanide deinsertion which takes place between intermediates **11** and **10**. To our knowledge an unambiguous example of isocyanide deinsertion has never been described before.[11b,c] Only in two examples, concerning Fe(η^5-cyclopentadienyl) complexes, has an isocyanide deinsertion been claimed.[11a,39] The reaction presented here is the first example in which the occurrence of an isocyanide deinsertion is unequivocally proven. In the [2.2.2] bicyclic tricarbonyl complex **3**, CO deinsertion has been found to compete to a small extent with isomerization toward complex **4**. When selectively labeled **3** (L′ = ^{13}CO) was kept at a temperature where it just starts to isomerize, then, in both the resulting **4** and unaltered **3**, the ^{13}CO label was found to be nonstatistically distributed over all possible positions, including the inserted position.[40b] This observation could only be rationalized by successive insertion and deinsertion reactions. With the present isocyanide complex **7a**, we now have found an example where the whole reaction sequence leading to the [2.2.2] bicyclic complex is smoothly reversible.

Formation of TMBC (8) and Fe(CNR)$_3$(tric) (9b,c). When the Fe(CNR)$_3$(*i*-Pr-DAB) complexes **6b,c**, containing aliphatic isocyanides, were treated with DMM, an organometallic compound, containing two coupled alkenes, and an organic dimer were formed. The (catalytic) coupling of unsaturated substrates by metal DAB complexes has already been described by tom Dieck et al.[3,13,41] Although at this moment the reaction and especially the mechanism are not completely understood and are being investigated further, the mechanism suggested in Scheme

(37) (a) Kawka, D.; Mues, P.; Vogel, E. *Angew. Chem., Int. Ed. Engl.* **1983**, *22*, 1003. (b) Marinetti, A.; Mathey, F. *J. Am. Chem. Soc.* **1982**, *104*, 4484. (c) Marinetti, A.; Mathey, F. *Organometallics* **1982**, *1*, 1488. (d) Wasserman, H. H.; Scheffer, J. R.; Cooper, J. L. *J. Am. Chem. Soc.* **1972**, *94*, 4991. (e) Sonolse, A. W.; Akasaka, T. *Tetrahedron Lett.* **1987**, *28*, 6653.

(38) Urove, G. A.; Welker, M. E.; Eaton, B. E. *J. Organomet. Chem.* **1990**, *384*, 105.

(39) (a) Yamamoto, Y.; Yamazaki, H. *Inorg. Chem.* **1974**, *13*, 2145. (b) Treichel, P. M.; Stenson, J. P. *Inorg. Chem.* **1969**, *8*, 2563.

(40) (a) Seils, F. Dissertation University of Duisburg, 1986; p 70. (b) *Ibid.*, p 98.

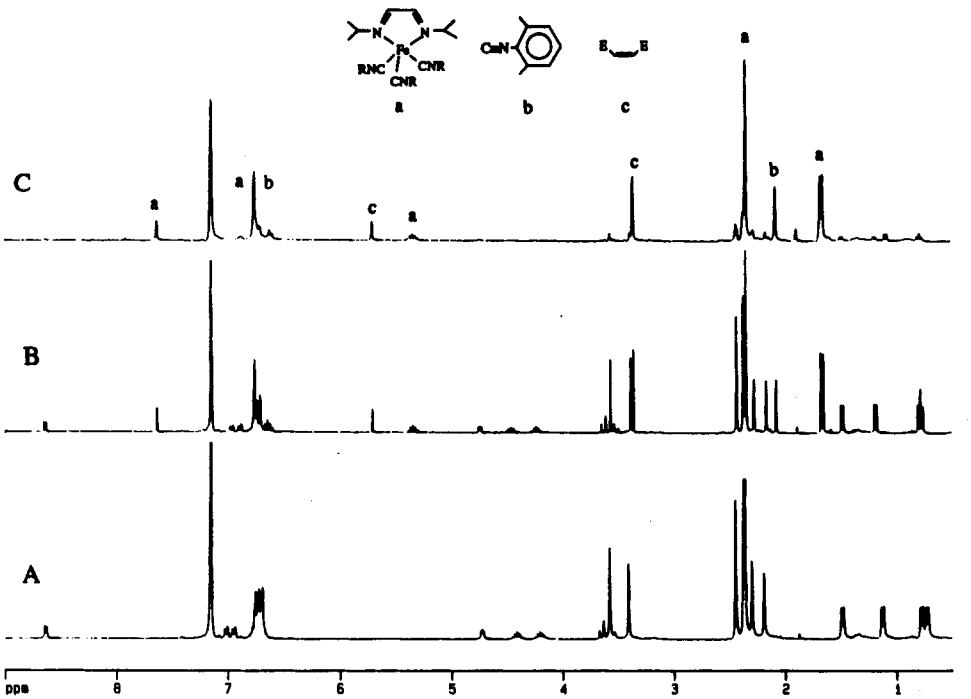

Figure 4. ^{1}H NMR spectra, recorded in C_6D_6 at 333 K within ca. 1.5 h, showing the disassembly of Fe(2,6-xylylNC)$_3$([2.2.2]bic) (**7a**) (spectrum A) to its starting components[34] (spectrum C).

Scheme III. Reversible Cycloaddition of Fe(2,6-xylylNC)$_3$(*i*-Pr-DAB) (6a) to DMM

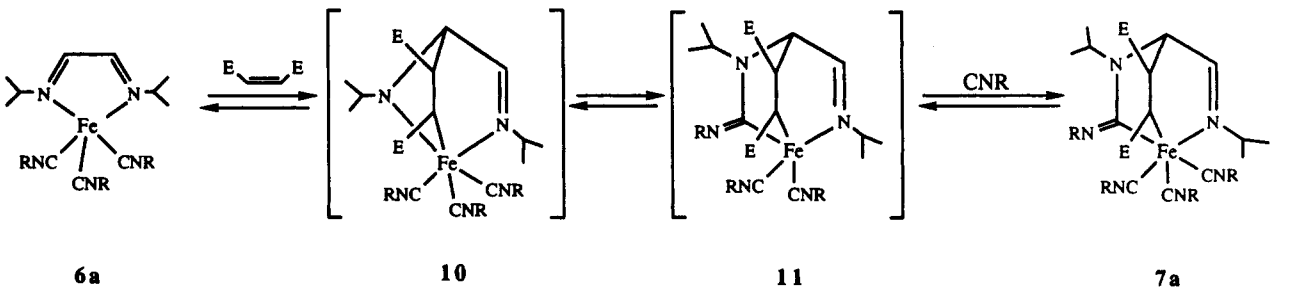

6a **10** **11** **7a**

IV can account for the formation of the observed products. The first step involves a substitution of an isocyanide ligand by an alkene, followed by the substitution of one imine group of the DAB ligand[42] by a second alkene, yielding intermediate **13**. Most likely first an electron-donating isocyanide will be displaced, considering the high electron density on the central metal atom. The presumption that the first steps are substitution reactions is supported by the observation that an excess of isocyanide remarkably slows down the reaction. The bis(alkene) intermediate **13** undergoes an oxidative coupling reaction followed by recoordination of the isocyanide, forming the metallacyclopentane **14**. From the literature many examples of metallacyclopentane complexes are known.[43] Although they are mostly reactive, Lindner et al. have described the single-crystal X-ray structure of a tricarbonyl(triphenylphosphine)ferracyclopentane.[43a,b,f] A β-H elimination from the metallacyclopentane intermediate **14** gives the hydride complex **15**. This β-H transfer requires a transition state in which the Fe–C–C–H dihedral angle is close to 0°.[43b-d] Although this requirement is not easily met by metallacyclopentane complexes, some examples are known.[43b,c,e] The σ-alkyl group in complex **15** undergoes a 1,3-proton shift of the β-proton to the terminal carbon atom of the alkyl group, creating a more stable internal double bond. Reductive elimination of the organic dimer TMBC (**8**) from intermediate **16** results in the regeneration of the starting complex Fe(CNR)$_3$(*i*-Pr-DAB) (**6b,c**), via a recoordination of the pendant imine group of the DAB ligand, closing a catalytic cycle. The occurrence of catalytic activity is supported by the fact that the mixture stays red during the course of the reaction, indicative of the continuous presence of Fe(CNR)$_3$(*i*-Pr-DAB). Efforts to perform a truly catalytic reaction with several turnovers, by the addition of more equivalents of

(41) (a) tom Dieck, H.; Diercks, R. *Z. Naturforsch.* **1984**, *39B*, 180. (b) tom Dieck, H.; Dietrich, J. *Angew. Chem., Int. Ed. Engl.* **1985**, *24*, 781. (c) tom Dieck, H.; Lauer, A. M.; Stamp, L.; Diercks, R. *J. Mol. Catal.* **1986**, *35*, 317. (d) tom Dieck, H.; Mallien, M.; Diercks, R. *J. Mol. Catal.* **1989**, *51*, 53.

(42) The substitution of a DAB ligand for an alkene has been suggested before: van der Poel, H.; van Koten, G.; van Stein, G. C. *J. Chem. Soc., Dalton Trans.* **1981**, 2166.

(43) (a) Lindner, E.; Schauss, E.; Hiller, W.; Fawzi, R. *Chem. Ber.* **1985**, *118*, 3915. (b) Lindner, E. *Adv. Organomet. Chem.* **1986**, *39*, 237. (c) McDermott, J. X.; Whitesides, G. M. *J. Am. Chem. Soc.* **1974**, *96*, 947. (d) McDermott, J. X.; White, J. F.; Whitesides, G. M. *J. Am. Chem. Soc.* **1973**, *95*, 4451. (e) Lauher, J. W.; Hoffmann, R. *J. Am. Chem. Soc.* **1976**, *98*, 1729. (f) Lindner, E.; Schauss, E.; Hiller, W.; Fawzi, R. *Angew. Chem.* **1984**, *96*, 727.

Scheme IV. Proposed Mechanism for the Formation of Fe(CNR)$_3$(tric) (9b,c) and TMBC (8)[a]

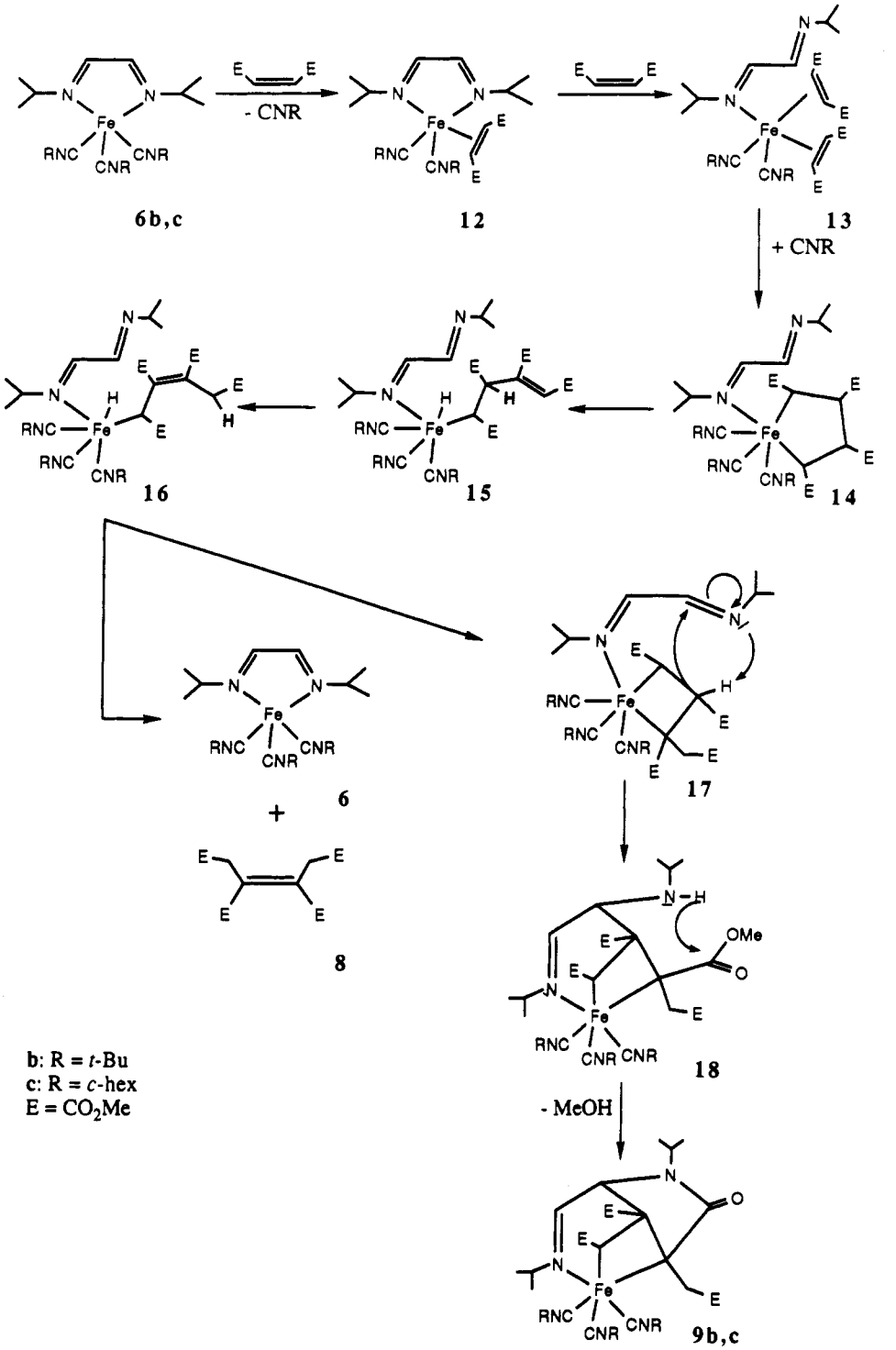

[a] Structures 12–18 are unobserved intermediates.

DMM, were impeded by the low rate of the reaction and the ready decomposition of the Fe(CNR)$_3$(*i*-Pr-DAB) starting complex. Further, a second competing reaction drains the catalytically active Fe(CNR)$_3$(*i*-Pr-DAB) molecules away or, rather, inhibits their regeneration. Besides a reductive elimination in **16**, the double bond in intermediate **16** can insert into the metal–hydride bond, forming the metallacyclobutane **17**. It is also possible to form complex **17** directly from intermediate **15** via an insertion of its double bond. In this case, however, the metal has to approach the more hindered carbon atom of the double bond, making this route less likely. As a consequence of the immediate vicinity of one and the presence of two more ester groups, one proton of the metallacyclobutane in complex **17** is rather acidic. This acidic proton is abstracted by the nitrogen lone pair of the uncoordinated DAB half, with concomitant attack of the remaining carbanion at the imine carbon atom and closure of the six-membered ring. For this step the uncoordinated imine group is essential. The lone pairs of coordinated imine units are used for binding to the metal; i.e., they are inaccessible for protonation reactions.[44] Finally, the

secondary amino group in 18 attacks the ester group, with elimination of methanol, forming the lactam ring of the isolated $Fe(CNR)_3$(tric) (**9b,c**).

Influence of the Isocyanide Ligands on the Course of the Reaction. The influence of the isocyanides on the reaction course is dramatic; the aromatic isocyanide gives rise to a bicyclic structure via a 1,3-dipolar cycloaddition, while with the aliphatic isocyanides an organic dimer and an organometallic tricyclic structure are found. A comparable diversity in products, depending on the type of isocyanide used, has been encountered before.[1b,9] And again, the difference in reactivity can only be explained electronically, not by the steric properties of the isocyanides. The reactivity and products of Scheme III, $Fe(CNR)_3$(tricyclus) (**9b,c**) and TBMC (8), are observed both with the smallest cyclohexyl isocyanide (remote cone angle[9b] 64°) and with the most bulky *tert*-butyl isocyanide (remote cone angle 76°), while with the aromatic isocyanide of intermediate bulkiness, 2,6-xylyl isocyanide (remote cone angle 69°), only the [2.2.2] bicyclic complex **7a** is formed. In the nearby cone angle approach, which takes the steric effects not only of the substituents but also of the C≡N fragment into consideration,[9b] all three isocyanides have equal angles of 102°. Obviously steric arguments are unable to explain the product distribution.

As stated earlier, the electron-donating aromatic isocyanide ligands enhance the electron density, making the Fe—N=C unit sufficiently reactive to undergo a 1,3-dipolar cycloaddition with an alkene. In comparison to the aromatic isocyanides, the aliphatic isocyanides in complexes **6b,c** create an even higher electron density at the metal, due to their inferior π-accepting capacities.[10,11,27] As a consequence of this large electron density at the metal and the weaker metal–isocyanide bond (less π backbonding), the substitution of one of the terminal aliphatic isocyanides by a better π-accepting alkene via a dissociative pathway becomes much faster than a cycloaddition reaction.

Diastereoselectivity. Both of the organometallic complexes, the [2.2.2] bicyclic complex **7a** and the tricyclic complexes **9b,c**, contain several chiral centers (five and six, respectively). In spite of the many possible diastereoisomers, IR and NMR spectroscopy point to the presence of only one diastereoisomer for either complex. Obviously, the formations of complexes **7a** and **9b,c** follow highly diastereoselective pathways.

Acknowledgment. Financial support from the Nederlandse organisatie voor Wetenschappelijk Onderzoek (NWO) and the Stichting Scheikundig Onderzoek in Nederland (SON) is gratefully acknowledged.

Supplementary Material Available: Tables of anisotropic thermal parameters, all H atom parameters, and bond lengths and angles involving H atoms and thermal motion ellipsoid plots for **7a**, 8, and **9b** (26 pages). Ordering information is given on any current masthead page. Listings of observed and calculated structure factor amplitudes (30, 10, and 41 pages for **7a**, 8, and **9b**, respectively) can be obtained from one of the authors (A.L.S.).

OM9204907

(44) The fact that the lone pairs of coordinated DAB ligands are not accessible for protons is also used for the elegant separation of the labile $Ru(CO)_3$(DAB) from free DAB. In the synthesis of $Ru(CO)_3$(DAB) from $Ru(CO)_5$ and DAB, the excess unreacted DAB was removed by washing with dilute aqueous acid, which causes protonation of the uncoordinated DAB and extraction into the aqueous layer.[45]

(45) Mul, W. P.; Elsevier, C. J.; Frühauf, H.-W.; Vrieze, K.; Pein, I.; Zoutberg, M. C.; Stam, C. H. *Inorg. Chem.* **1990**, *29*, 2336.

(46) For presently unknown reasons, the isocyanide-containing complexes tend to give notoriously bad elemental analyses, in particular for carbon.[1b,9b,27f]